IMPLICATIONS OF MODERN OBSERVATIONS ON SOLAR FLARE THEORY

IMPLICACIONES DE LAS OBSERVACIONES MODERNAS EN LA TEORIA DE LAS FULGURACIONES SOLARES

Cristina H. Mandrini
Instituto de Astronomia y Fisica del Espacio

and

Marcos E. Machado
Observatorio de Fisica Cosmica - CNIE

RESUMEN: Describimos, en forma general, la fenomenologia de las fulguraciones solares a traves de diversos aspectos: una revision breve de la historia de las observaciones, una descripcion general de sus caracteristicas observadas y, por ultimo, una enumeracion de los requisitos basicos que deben satisfacer los modelos de fulguracion. En segundo termino, resumimos algunos de nuestros resultados recientes referidos a las caracteristicas de la liberacion de energia observadas en eventos que abarcan un rango, tanto espacial como energetico, muy amplio: fulguraciones, microfulguraciones y abrillantamientos de gran escala. La base de nuestro analisis es el conjunto de datos, unicos en su tipo, obtenidos por el Espectrometro de Imagenes en Rayos X Duros que volo a bordo del satelite Mision para el Maximo Solar y magnetogramas vectoriales del Centro de Vuelos Espaciales Marshall.

1 Fellow of the CONICET

ABSTRACT: We present, in general, the solar flare phenomenon going through several aspects: a brief historical survey of solar flare observations, a general description of its observed characteristics and, finally, an account of the basic requirements set on solar flare models by the observational data. As a second step, we summarize some of our recent results on the observed character of energy release in a vast energetic and spatial range of events: flares, microflares and large scale brightenings. The base of our analysis is the unique set of data provided by the Hard X-ray Imaging Spectrometer, that flew aboard Solar Maximum Mission satellite, and ground-based vector magnetograms from the Marshall Space Flight Center.

1. INTRODUCTION

1.1 A little history

Solar flares are energy release transient phenomena, the most spectacular and violent ($\geq 10^{32}$ erg in $\simeq 10^{2} - 10^{3}$ s, in extreme cases) form of activity in the sun atmosphere.

On September 1, 1859, R.C. Carrington (1860) and R. Hodgson (1860) observed for the first time a white light flare, being this type of event not the most common within these phenomena. From then on, and until the launching of the Orbiting Solar Obsevatory (OSO) satellites, the data were obtained mainly from earth in several wavelengths. There exists an overwhelming quantity of obeservations, mainly in Hα, which have been the basement for general conclusions about the size, shape, intensity, etc. of flares. In particular, these events have been classified according to the area covered and intensity observed in this wavelength (see e.g. Svestka, 1976). This classification describes quite well the coldest region of a flare ($T \simeq 6 - 8\ 10^{3}$ K) and its levels of importance are related to certain effects induced in earth, such as: geomagnetic storms and auroras.

However, as Parker has said: "trying to understand the basic physical processes at work in flares using only Hα data, is the same like trying to describe a dinosaur looking only at its footprints". In this line, the analysis of a hotter ($T \geq 10^6$ K) emission component, that has come evident in modern observations, has thrown light in the understanding of the physics of flares.

It is known, from long time ago, that almost all flares develop in active regions (ARs) with sunspots and that they are more frequent as more complex the sunspot group is (Bell and Glazer, 1959; Dodson and Hedeman, 1970). It has also been observed that the events that take place in the penumbral part of a sunspot release the largest amounts of energy (see review works by Švestka, 1968, 1981 and studies by Dodson and Hedeman, 1960; Ellison et al., 1961; Martres and Pick, 1962; Neidig, 1977; Dwivedi et al., 1984). However, the first observations showed that flares do not appear in the umbra (Svestka et al., 1961), being evident that there are other important aspects in the magnetic configuration besides the field intensity. With the advent of the solar magnetograph designed by Babcock in 1953, it was possible to compare directly the photospheric magnetic field and the region of the flare. Its location with respect to the longitudinal neutral line ($B_{11} = 0$) was studied by Martres et al. (1966) and Moreton and Severny (1968), who related it with the presence of small bright Hα points; these appeared at both sides of $B_{11} = 0$ at the beginning of the event in regions of intense field gradient. Though the first data provided information of the longitudinal magnetic field only, it was possible to infer, under certain assumptions, the direction of the transverse component (Zvereva and Severny, 1970). Zirin and Tanaka (1973) and Tanaka and Nakagawa (1973) were the first to discuss the importance of the observed magnetic shear in the structure where the events develop. Magnetic shear gives the idea of the departure of the local magnetic field from a potential configuration; being the shear angle, defined by Hagyard et al.

(1984), the angular difference between the observed and the potential field direction calculated from longitudinal field measurements. We will discuss this point in relation to the energy released by individual bipoles in the following Section.

There are observations of two types of phenomena that point out the essential role of the magnetic field structure and dynamics. These are: sympathetic and homologous flares. Almost simultaneous events, called sympathetic, are often observed in different active regions (Richardson, 1936, 1951; Becker, 1958; Moreton and Ramsey, 1960; Valnizék, 1961; Athay and Moreton, 1961) the interconnecting loops seem to be the channels through which different types of perturbations can travel from one active region to another giving place to this phenomenon. On the other hand, it is frequently seen that one event happens in the same place and preserving the same geometry as a previous one. This recurring character of flares was observed for the first time by Waldmeier (1938) and shows that: either the non-potential configuration is rebuilt after every event, or only a part of the stored energy is released after every event.

It was during the 60's that considerable progress was made in the observational area. The data obtained from satellites gave the chance of analyzing flares in wavelengths not yet detected from earth. The first soft X-ray observations were provided by the instruments aboard OSO-1 (White, 1964). The spectrometers on OSO-3 (Hudson et al., 1969), OGO-5 (Orbiting Geophysical Observatory, Kane and Anderson, 1970) and OSO-7 (Datlowe et al., 1974a,b) observed innumerable small events between 5 keV to $\simeq$ 100 keV. These data were used mainly for statistical studies. In the EUV, the first data with spatial resolution were those of the instrument of the Harvard College Observatory (300-1350 Å) aboard OSO-4 and OSO-6 (Wood et al., 1972). Comparing these observations with those obtained simultaneously in X-rays by other satellites, Wood and Noyes (1972) concluded that the EUV emission was a combination of two components: the first associated

to the non-thermal and impulsive X-ray radiation, that would result after the injection of accelerated electrons in the dense chromosphere during the flare triggering and the second related to the thermal X-ray emission, that would come from the indirect heating of the chromospheric plasma due to a coronal source.

These early USA satellite experiments were complemented by the TD-1A of the European Space Research Organization in 1972; its hard X-ray spectrometer (Van Beek, 1973) observed the solar radiation between 25 keV and 1050 keV with high temporal resolution. Hoyng et al. (1976) analyzed thoroughly the data in relation to the source models for hard X-ray emission during flares.

Skylab was the first manned mission that observed the Sun (1973 - 1974). This space station had 8 telescopes (Apollo Telescope Mount, ATM) covering a wide wavelenght range (2-7000), which allowed to obtain information of the different zones in the solar atmosphere. A review of the observations and most important conclusions of ATM can be found in Zirker (1977), Sturrock (1980a) and Orrall (1981); though, perhaps, the outstanding result of this mission was the recognizance that the classic picture of a homogeneous corona heated by sound waves is, at most, a minor component. The solar corona is structured in a vast hierarchy of magnetic loops, playing the magnetic field an essential role in the heating of the external solar atmosphere (see Kuperus et al., 1981 for a review). On the other hand, regions of open field lines show reduced coronal emission and are the sites where the solar wind originates.

Though Skylab was launched during the minimum of the solar cycle, a substantial leap forward in flare modelling took place after its high spatial resolution X-ray and UV pictures. In particular, flares were seen like very bright coronal loops that could come in two main classes, distinguished by the global form and action of the magnetic field in which they occurred (Pallavicini et al., 1977; Moore et al., 1980). In one class, the flare develops within the loops of a

single bipole, loops that remain closed throughout the event. In the other class, the flare occurs in a sheared magnetic arcade as an integral part of the eruption and expulsion of the magnetic field carried in a filament and coronal mass ejection. Moore et al. (1980) referred to the above two classes as "compact" and "two-ribbon" flares. Following Švestka (1986), we shall call the first class "confined" and the other "ejective", according in this last case with the terminology in Machado et al. (1988a); we do this so as to emphasize the essential differences between both.

After this mission we can mention: the International Sun Earth Explorer (ISEE, 1978) and P78-1 (1979) satellites. The first spacecraft carried aboard a hard X-ray spectrometer observing between 26 and 3170 keV (Kane et al., 1979); the results obtained, relevant to flares, can be found in Kane (1983). In relation with P78-1, Doschek (1983a) describes the instruments aboard and Doschek (1983b) summarizes the conclusions derived from these data.

Besides the numerous satellite experiments already mentioned, a great deal of information was provided during the same period by instruments that flew in balloons. All these data, compiled along almost 20 years, were surpassed in quality in some cases and complemented in others by the observations of the Solar Maximum Mission (SMM). This USA satellite, together with Hinotori from Japan, were the last two devoted, almost exclusively, to the observation of solar flares. Kondo (1983) and Tanaka (1983, 1987) describe the intrumentation and the main results from Hinotori, respectively.

SMM was launched on February 14, 1980, near the maximum of solar cycle Nº 21. In November 1980, the spacecraft attitude control system failed; being repaired in orbit by the crew of the Space Shuttle in November 1984. The satellite de-orbited and was

lost on December 2, 1989 in the Indian Ocean. During its useful life, more than 400 papers based on SMM observations and their interpretation have appeared in scientific journals. A compilation of SMM results can be found in Kundu and Woodgate (1986), while Solar Physics Nº 65 was devoted exclusively to a description of the instruments aboard.

We shall now outline briefly the main features of the Hard X-ray Imaging Spectrometer (HXIS, Van Beek et al., 1980), since its observations are the basis of our next analysis. Two dimensional imaging in hard X-ray of flares became possible for the first time with HXIS. This instrument consisted of an imaging collimator of ten grid plates divided into 576 sections and a position sensitive detector system. The grids formed a coarse field of view (CFOV) 6′ 24′′ in extent (with 32′′ resolution square picture elements or "pixels") and a fine field of view (FFOV) of 2′ 40′′ (with 8′′ resolution pixels). Every pixel was observed, with time resolution down to 1.25 s and up to 7 s depending on the operational mode, in six energy bands ranging from 3.5 to 30 keV and arranged in the following way: B1 3.5-5.5 keV, B2 5.5-8.0 keV, B3 8.0-11.5 keV, B4 11.5-16.0 keV, B5 16.0-22.0 keV and B6 22.0-30.0 keV. Though HXIS had only nine months of active operation its data set constitutes a unique record of solar flares, with a spatial resolution never before achieved at those high energies.

In this survey we have emphasized the observations that have been more relevant for solar flare theory. At present, several satellite experiments are being prepared to fly during this solar cycle (see Rovira, 1990) which will try to throw light in several points that still remain obscure, not only in relation to flares but also in many other aspects of solar physics.

1.2 Basic description of flare spectrum

Solar flares emit radiation in a wide range of wavelengths. In Figure 1 we show the temporal evolution of a typical flare; it can be seen that, though there exists a general agreement, the light curves are different enough so that no one alone can completely describe the event.

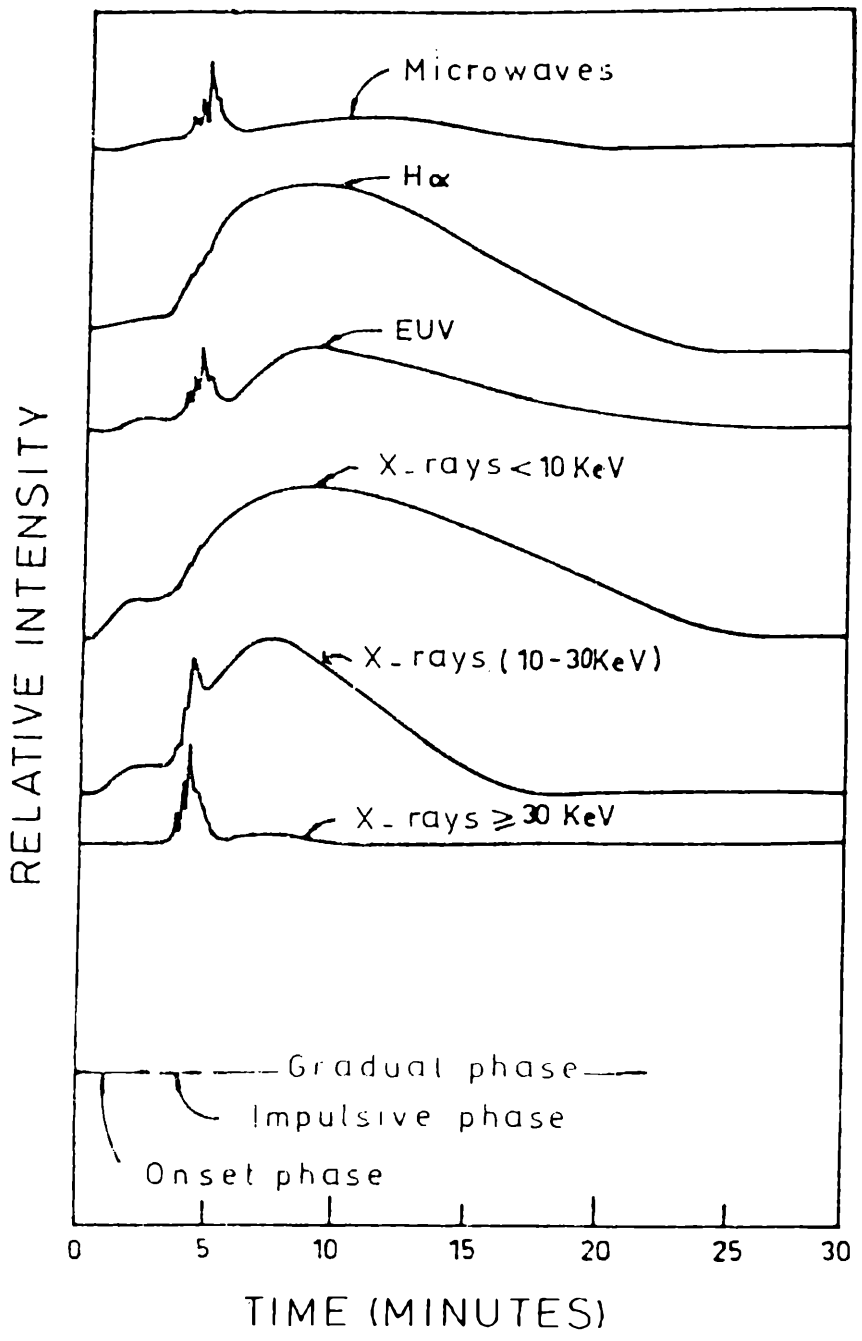

Fig. 1 Intensity as a function of time at different wavelengths for a typical flare. We have indicated the phases in which the X-ray emission is divided.

Some flares may also eject plasma into the corona and the interplanetary space originating a shock wave. As this wave travels, it excites plasma oscillations that give place to a type II burst, a drifting radio emission. Part of the electrons that have been accelerated during the flare stay trapped behind the shock producing, through gyrosynchrotron radiation, a metric radio continuum called type IV radio burst. This emission can be stationary or moving, either if it comes from the electrons that stay in zones of closed magnetic field lines or from those that are in the ascending plasma cloud.

The temporal evolution of the observed intensity in different wavelengths is often divided in phases that are related, in first approximation, with distinct physical processes. In the X-ray range (see Fig. 1), we shall talk of: onset, impulsive and gradual phases (see Machado et al., 1988a). The onset phase indicates the beginning of the event with a slow rise in soft X-rays. This phase can, eventually, appear in hard X-rays. Afterwards an impulsive phase is observed in hard X-rays, during this period the soft X-ray light curve has not reached its maximum but shows a steep slope. The gradual phase, that may not be present in many events, follows the impulsive in hard X-rays. In the soft X-ray curve, the period after the maximum is often called main phase (see e.g. Priest, 1982).

1.3 Basic requirements for flare models

The theoretical interpretation of solar flares has been the subject of long discussions in the last years, and the great number of models that have appeared do not explain the flare phenomenon in all its aspects. Most of these are qualitative in nature and agree with observations in a general way. Some of the basic physical parameters used in models, as e.g. the size scale of the

energy release zone, are orders of magnitude smaller than the minimum instrumental spatial resolution ever achieved and, therefore, direct comparison between observations and theory is not yet possible. On the other hand, the flare observables are the result of the convolution of the primary energy release characteristics with those of the environment where the flare occurs, through a combination of plasma instabilities and energy transport processes. Despite all these constraints, observations obtained in the last two decades have been substantial for flare theory.

The problem of flare model requirements is not a completely objective matter, and a discussion giving different weight to certain aspects of flare phenomenon can be found in different reviews about solar flare models (Sturrock, 1980b; Spicer and Brown, 1981). We point out that the requirements we enumerate here, are the basic ones that emerge from the analysis presented in the next Section.

All the hypothesis that are made about the nature of solar flares give an important role to the magnetic field of solar active regions, as can be inferred from the observations described previously. It is accepted, in general, that a solar flare is a coronal phenomenon and that the energy released is stored in stressed (current-carrying) magnetic structures; being the energy storage process one of the points that has to be considered.

Provided that the coronal and photospheric plasma is highly conducting, the most straightforward way of increasing the energy content of a coronal potential configuration, where $\beta \ll 1$ (β, ratio of the gas pressure to the magnetic pressure), is through the motion of the photospheric ($\beta \gg 1$) footpoints of magnetic loops. This energy storage can be considered as a slow process along which the magnetic field evolves through a succesion of force-free configurations, ending up in a higher energy state (Low, 1982).

This process seems to be possible since the photospheric motions timescale is of the order of days, while the coronal field would adjust to this perturbation, with the Alfven velocity, in a timescale of the order of seconds. Figure 2 shows the way in which the original configuration can be deformed: a whirling velocity field can twist the footpoints of a loop (upper drawing) or an arcade can be sheared due to motions tangent to $B_{11} = 0$ (lower drawing).

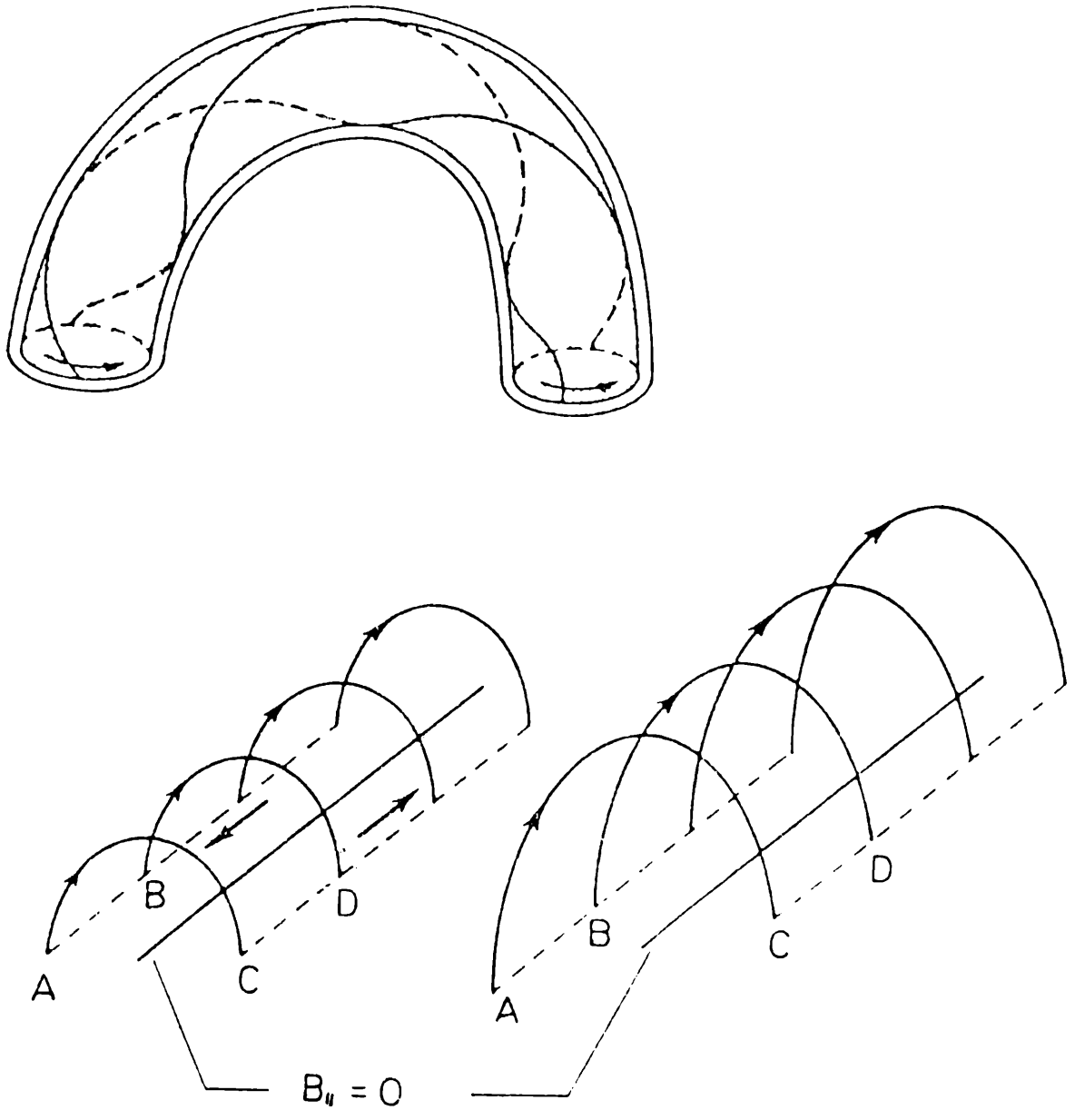

Fig. 2 Schematic representation of the deformation of potential coronal fields due to footpoint motions: a twisted loop (upper drawing) and a sheared arcade of loops (lower drawing).

McClymont and Fisher (1989) evaluate the mechanic energy associated to the turbulent motions of the upper convective zone. They find out that the energy needed for a flare cannot be instantaneously provided, but that along $\simeq$ 1 day a flux tube would store 10^{31} erg. In his model of coronal heating, Parker (1981a,b, 1983a,b) proposes that footpoint motions continuously drive the coronal magnetic field into states of dynamical nonequilibrium. In this process, many discontinuities (current sheets) are spontaneously formed; in these regions the field reconnects enhancing, thus, Joule dissipation and simplifying the magnetic structure. However, Antiochos (1987) shows that for continuous boundary conditions only continuous solutions are allowed for the coronal force-free fields; being thus not proved Parker's assertion. There are also coronal heating models based on the excitation of magnetohydrodynamic (MHD) turbulence (van Ballegooijen, 1986; Gomez and Ferro Fontan, 1988); according to them, the energy coming from photospheric motions undergoes a cascade process towards the microscale where it is efficiently dissipated through Joule effect. These models are stationary and do not take into account an eventual energy storage. At this point, the problem of explaining through the same process coronal heating and energy storage for a flare has not yet been solved.

The observation of photospheric magnetic shear along longitudinal neutral lines (Krall et al., 1982; Hagyard, 1988) suggests the existence of net currents flowing from the photosphere towards the corona and, on the other hand, the fact that the longitudinal magnetic configuration of an active region does not change after a flare (remember also homologous flares) indicates that the energy released is energy in excess over the potential one. Our results also suggest that, differences in the energetic evolution of independent bipoles are due to different levels of energy storage (see next Section).

Most of flare models (see however Henoux and Somov, 1987) do not consider the energy storage process and assume that energy is already available in the coronal loops.

The coronal field deformation, just described, is an ongoing process. However, it is not expected that the magnetic stresses can increase indefinitely. Models that study sequence of force-free equilibria in arcades (as those shown in Figure 2) find that the structure eventually reaches a metastable state (Birn and Schindler, 1981) and infer that, at this moment and due to some perturbation, the flare is triggered, the configuration releases its free energy and returns to a low energy state. The presence of an impulsive phase at the beginning of the emission in certain wavelengths shows that the energy release is violent. A flare model must then consider a flare triggering mechanism. Those that propose that the geometry of the event is given by more than one bipole, assume that the interaction between them starts the energy release (see e.g. Heyvaerts et al., 1977); while those that consider that flares take place within one closed loop, propose the development of some type of instability (see e.g. Spicer, 1977; Van Hoven, 1976, 1981). Our results support both the idea that the interaction between bipoles, probably through reconnention, occurs at the beginning of most flares and the idea that the bulk of energy release takes place within the bipoles (see next Section).

Another problem that flare models have to explain, is that of the energy release mechanism. In particular, the impulsive phase seems to be the one that sets the major requirements. During this period, the observations indicate the presence of high energy accelerated particles and, therefore, the proposed mechanism has to be able of heating the plasma and accelerating particles. For example, the hard X-ray emission requires, according to the assumed source model, either the presence of zones with $T > 10^8$ K (Brown et al., 1979; Smith and Lilliequist, 1979) or the acceleration of

$\gtrsim 10^{36}$ electrons s^{-1} (Hoyng et al., 1976). Most of modern flare models consider magnetic reconnection or annihilation in current sheets as the energy release mechanism, being then the topology of the reconnecting region what characterizes the model. Excellent reviews of flare models are those by Sturrock (1980b) and Spicer and Brown (1981).

2. FLARE AND FLARE-LIKE PHENOMENA IN MAGNETICALLY COMPLEX ACTIVE REGIONS

In recent works (Machado et al., 1988a,b; Mandrini et al., 1989; Mandrini and Machado, 1990) we have analized the properties of flares and other associated phenomena that are determined from HXIS data and combined ground-based observations of the magnetic field. In our analysis we have considered the soft and hard X-ray spatiotemporal evolution, the time dependence of the thermal energy content in different magnetic bipoles participating in the flares and the relationship of the X-ray behaviour to the strength and observable shear of the magnetic field. Our aim with this study has been to draw a picture of flares meaningful for the understanding of the energy release process and the field topology where they occur, confirming and/or adding to the findings of previous observations, i.e. those of the Skylab. In this Section we summarize and illustrate our main results.

We point out that we take as a working premise that the hard X-ray emission at photon energies $\varepsilon \geq$ 16 keV is intrinsically associated with the primary energy release process, irrespective of whether the bremsstrahlung emission at such energies is thermal non-thermal or a combination of both. This premise is based on the fact that the highest energy release powers (erg^{-1} s) are those needed to explain the observations during the hard X-ray burst, whatever the source of this emission is (see Machado, 1982; Vlahos et

al., 1986 for reviews). The limit $\varepsilon = 16$ keV to the hard x-ray emission is set only for instrumental reasons, since it is the inferior boundary of the lowest energy band (B5) of HXIS that is not severely contaminated by radiation from the ($T \simeq 10^7$ K) soft x-ray emitting plasma.

2.1 Confined and ejective events

Machado et al. (1988a) included in their analysis of flare properties 23 events from HXIS data set. Here we describe, in particular, three flares showing similar morphological characteristics that developed in AR 2779 (NOAA number) during November 1980, and then extend our conclusions to some other examples from the original list (see Table I in Machado et al., 1988a).

In Figure 3 we show the evolution of the overall magnetic field of AR 2779 between Nov. 6 and 12, 1980. It can be seen that the positive polarity regions appears split towards the E (central magnetogram), with respect to the original configuration (upper magnetogram), evolving to the situation in which the analyzed events took place (lower magnetogram). AR 2779 was composed of two main sunspots with a reversed polarity region between them (see Fig. 3 and Fig. 4a). In Figure 4c we give a schematic representation of the coronal field lines across the neutral lines labelled as A, B and C (Fig. 4b), plus a large structure D which connects the leading and trailing spots. Such configuration should have and X-type neutral point region above the intermediate neutral line A, which we have encircled in Figure 4c. This line was the region with the largest observable magnetic shear along the period shown in Figure 3; according to Hagyard et al. (1984) the maximum shear angle exceeded 70 .

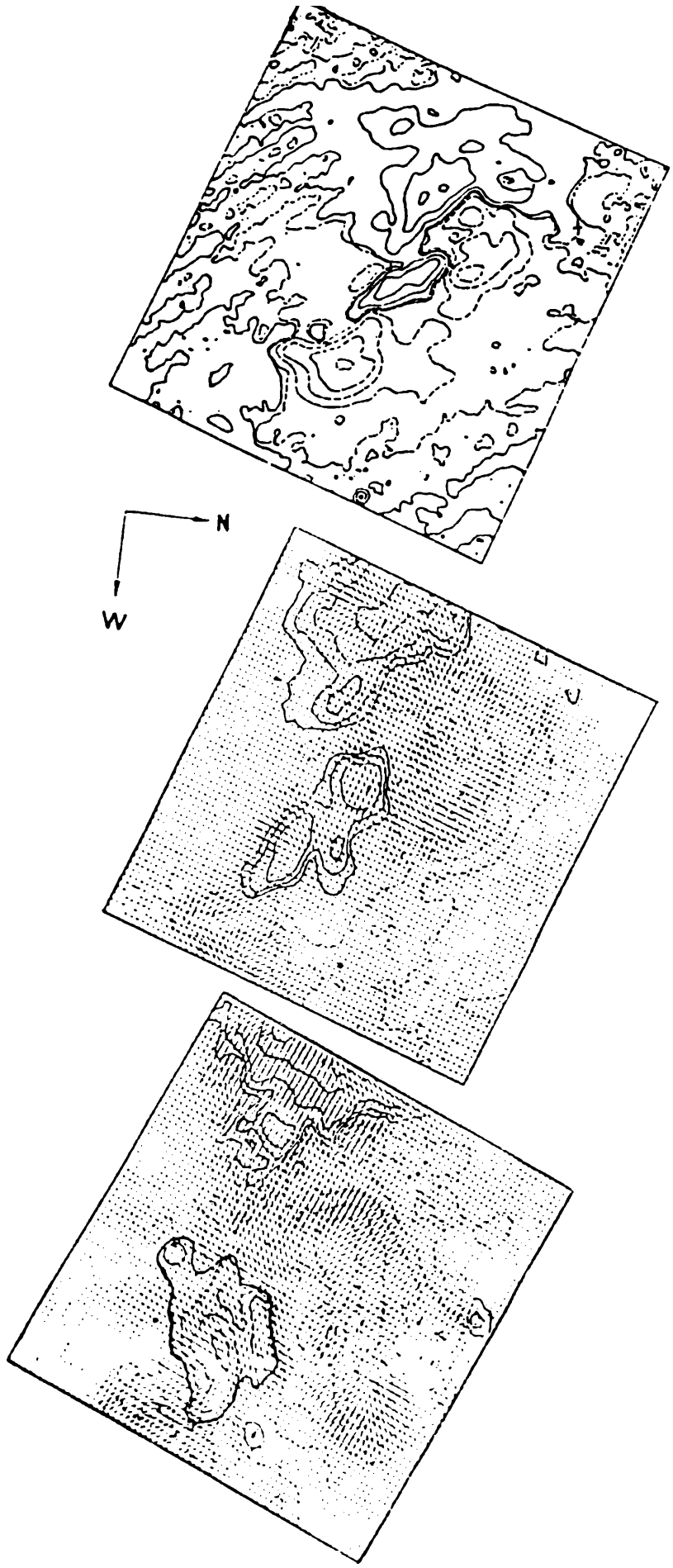

Fig. 3 Temporal evolution of the magnetic field of AR 2779. Longitudinal magnetogram obtained on Nov. 7, 1980, positive polarity is shown with filled lines and negative with dashes (upper figure). Overlay of longitudinal and transverse field measurements of Nov. 8 (central figure) and Nov. 11, 1980 (lower figure). Notice that neutral line A (Fig. 4) is a region of intense magnetic shear. All magnetograms were obtained at the Marshall Space Flight Center (MSFC).

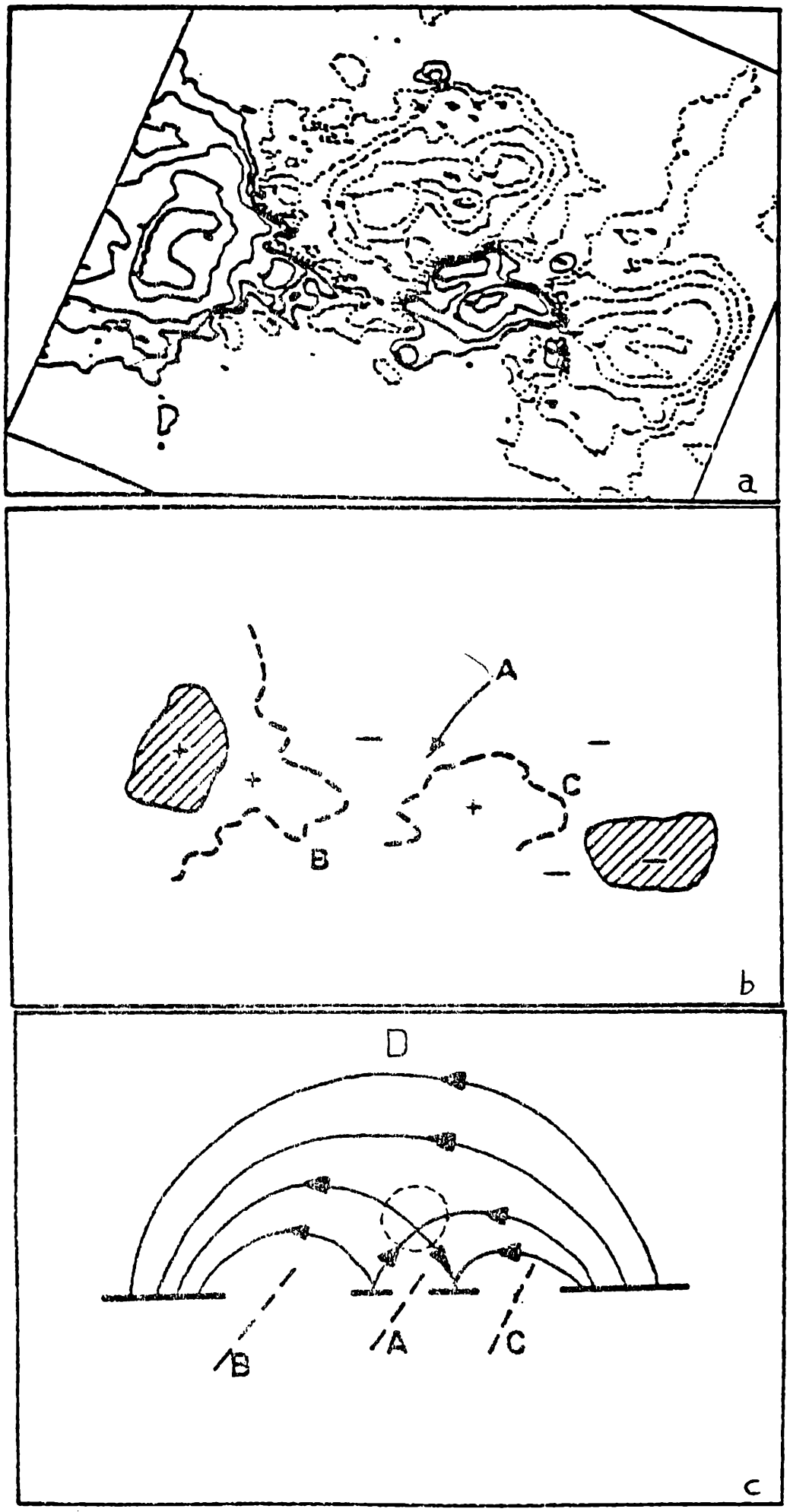

Fig. 4 a) Longitudinal magnetogram of AR 2779 obtained on Nov. 11, 1980, this has been rotated 90 with respect to Fig. 3. b) Neutral lines diagram. c) A 2-D sketch of the coronal field of AR 2779.

Figure 5 depicts the soft and hard X-ray light curves for the three events. The impulsive phase, marked with a bar, is characterized by the hardest X-ray spectrum (largest flux of high energy, $\varepsilon > 100$ keV, photons) in the Hard X-ray Burst Spectrometer (HXRBS, Orwig et al., 1980) data (Dennis, 1987); this indicates the generation and precipitation of high energy electrons (Emslie and Machado, 1987). After the impulsive spike, a gradual phase is clearly seen in Nov. 11 flare; being also present, though less intense, in HXRBS data for the other two events. This component has a softer spectrum.

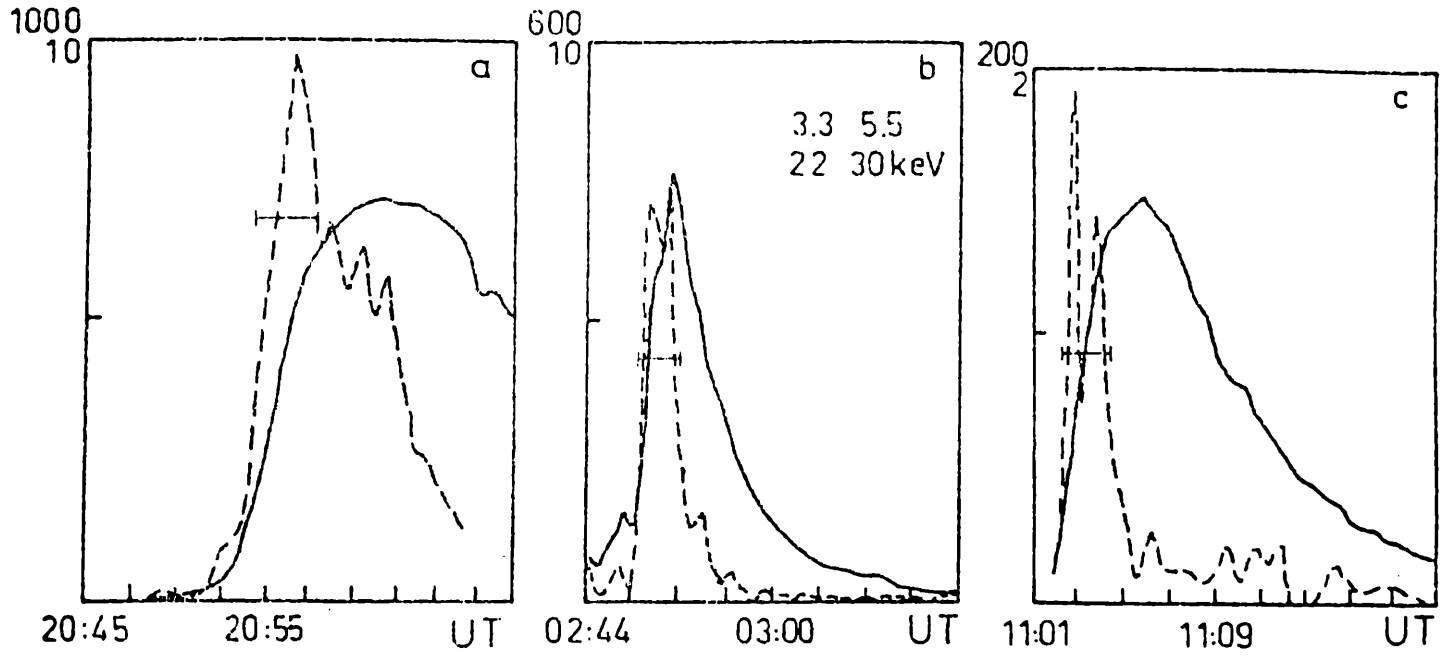

Fig. 5 Soft (filled line) and hard (dashes) X-ray light curves for the flares analyzed in AR 2779: a) Nov. 11, 20:52 UT, b) Nov. 12, 02:42 UT and c) Nov. 12, 11:00 UT events. Tops of the scales (upper left corner) correspond to the soft (top) and hard (below) X-ray c s^{-1}.

Figures 6, 7 and 8 show the spatial development of the emission seen by the HXIS low energy bands as a function of time; here we have outlined the neutral lines A and B (see Fig. 4). A small and bright zone, labelled F1 in the three cases, is observed over neutral line A. This region is surrounded by other two: one extending towards the NW (F3) and another, much more elongated, towards the E-NE (F2). According to the location relative to the

neutral lines, the identified zones correspond to three independent bipoles. The earliest flare emission site was located within the intermediate region (F1) of highly stressed field (see Fig. 3).

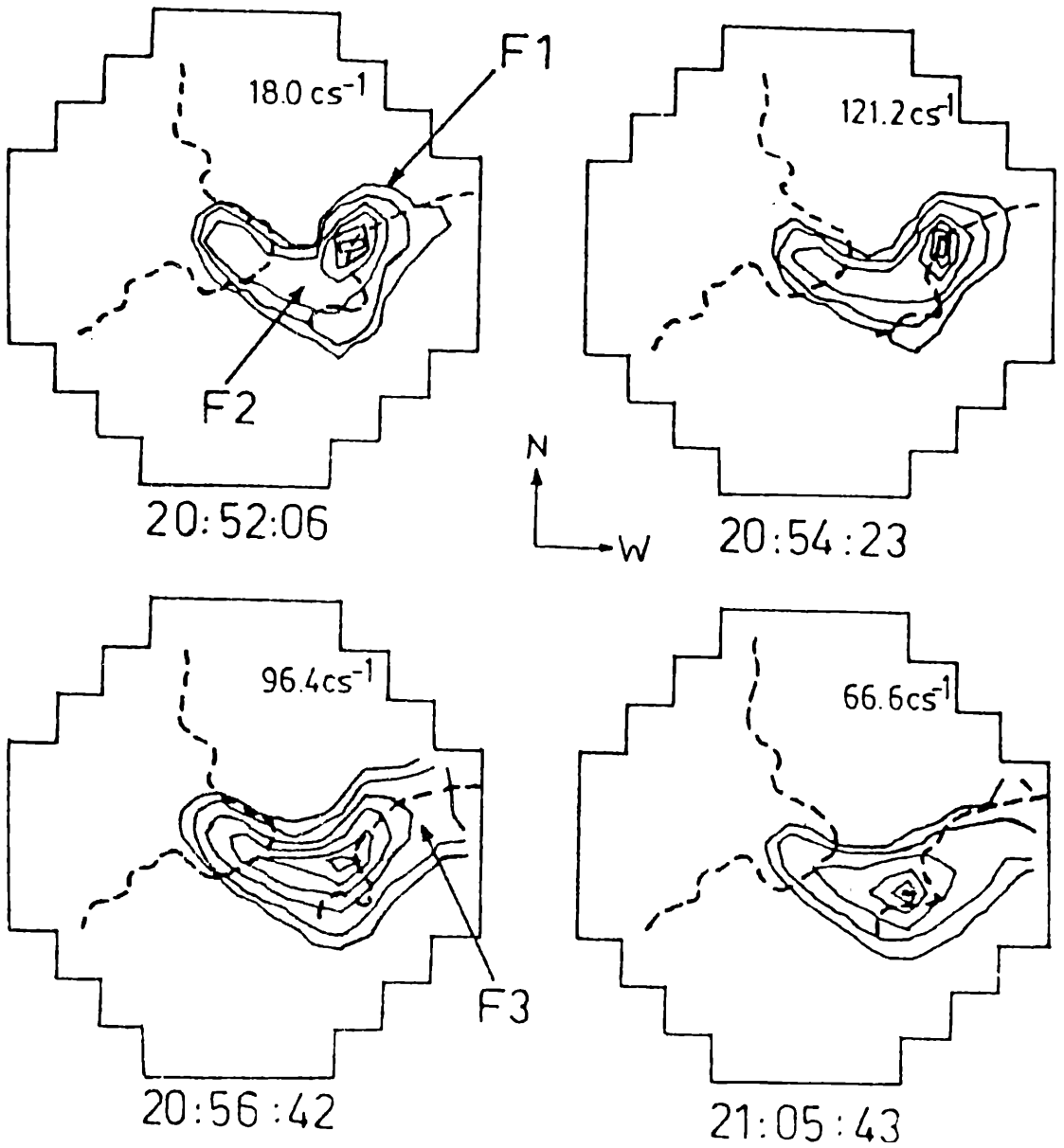

Fig. 6 3.5 - 8.0 keV images in the HXIS FOV for Nov. 11 flare. Every step is equal to 16" in the Sun. The contours correspond to: 90, 75, 50, 25, 10 and 5% of the maximum number of counts which is noted within HXIS field. The number below every figure is the corresponding UT. We have superimposed neutral lines A and B (see Fig. 4).

Subsequently, the emission expanded into F2 and F3 in close association with the development of the impulsive phase, this suggests strong interaction between the bipoles. This behaviour is seen better in Figures 9a, 10a and 11a, where we show the soft X-ray light curves

and the thermal energy (Eth = 3k T $Y^{1/2}$ $V^{1/2}$ [erg], where Y is the emission measure and V the volume) evolution for the three structures. It can also be noticed (see Fig. 6, 7 and 8 too) that at flare maximum F2 is the predominant source; note in Figure 3 that this structure extended over a neutral line with observable magnetic shear. Regarding the hard X-ray (16 - 30 keV) emission, the compact F1 bipole is the most important structure towards the beginning of the impulsive phase; while the bulk of this emission is concentrated only over F2 during the gradual phase (see, as an example, Fig. 12).

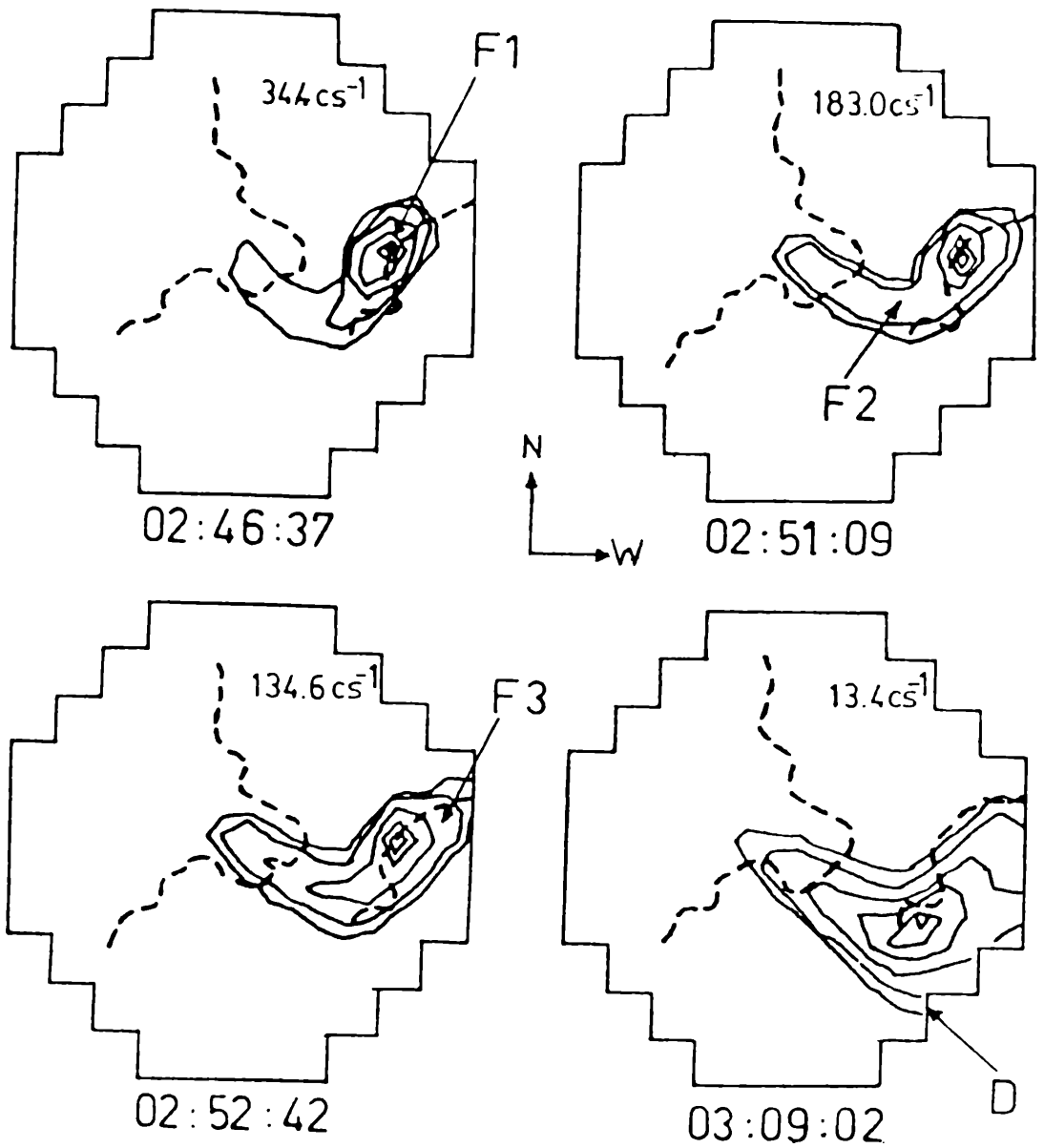

Fig. 7 Idem Fig. 6 for Nov. 12, 02:42 UT flare. Notice the location of the large scale structure D in the last image.

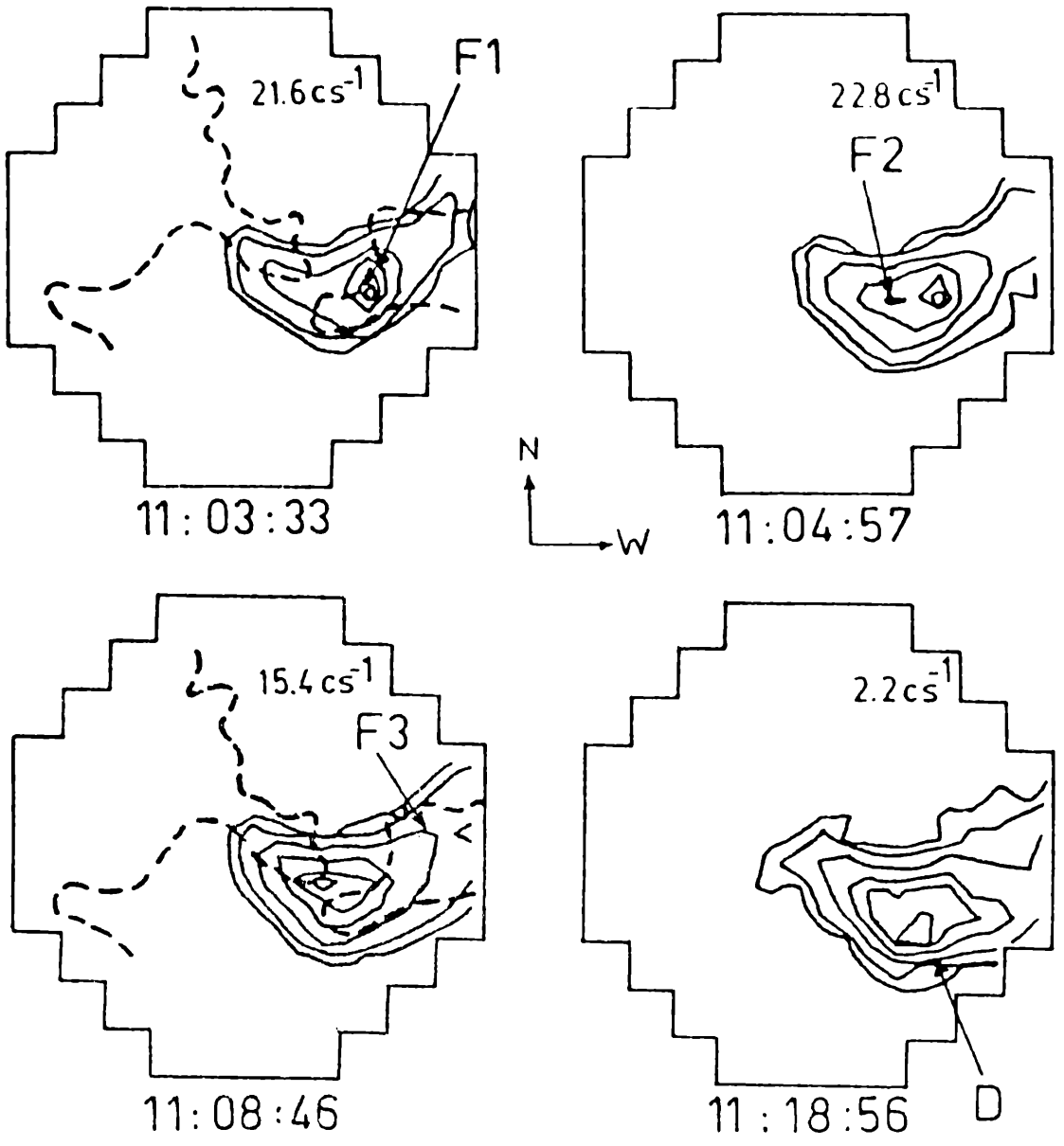

Fig. 8 Idem Fig. 6 for Nov. 12, 11:00 UT flare. We have indicated the position of D in the last image.

We can now compare the characteristics of the hard X-ray burst emission with the temporal variation of Eth in every region. As it can be noticed from Figures 9b, 10b and 11b, Eth for F1 reaches its maximum and also starts decaying slightly before the end of the impulsive phase. The slopes of these curves are quite steep at both sides of their maximum, being this behaviour consistent with the evolution of the soft X-ray emission within this bipolar structure. In the case of F2 and F3, the larger values of dEth/dt are observed

during the impulsive peaks; this agrees with our previous statement that this phase is characterized by the spread of the emission over the two structures. It is however quite clear that after this initial rise the behaviour of F2 and F3 is clearly different. This is particularly evident in the case of the Nov. 11 and Nov. 12, 11:00 UT flares, where we see that Eth(F2) continues rising $\simeq$ 5 m after the impulsive peak; while Eth(F3) reaches a plateau during this period. The evolution of the Nov. 12, 02:42 UT event is slightly more complicated due to the considerable level of preburst activity (de Jager and Boelee, 1984; Cheng et al., 1985), but still the same type of behaviour can be recognized.

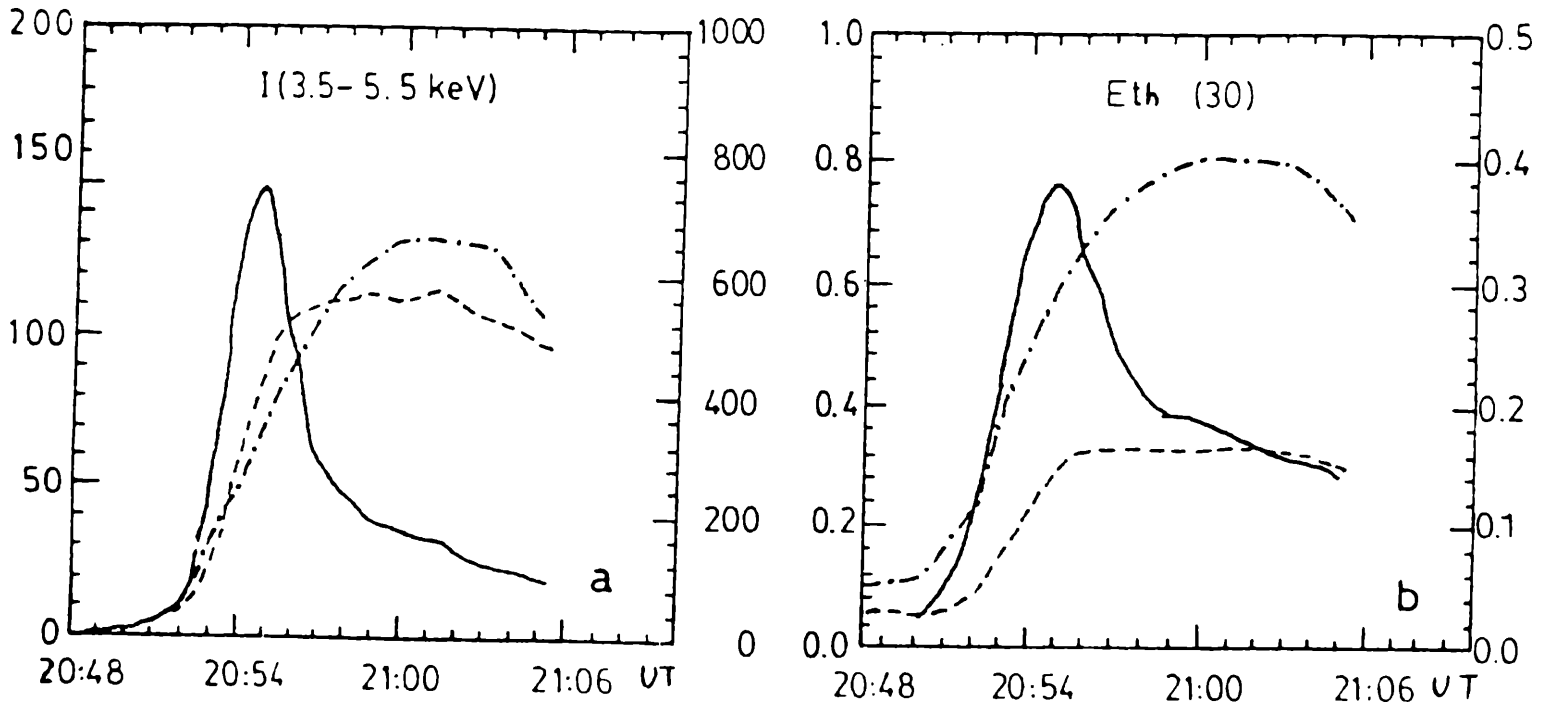

Fig. 9 Nov. 11, 20:52 UT flare. a) Intensity (c g) as a function of time for F1 ( ), F2 (-.-) and F3 (---). The left vertical axis corresponds to F1 and F3 and the right to F2. b) Thermal energy evolution in units of 10 erg. The left vertical axis corresponds to F2 and F3 and the right to F1. The volumen chosen for every structure is V = 10 cm just to establish a frame of reference. T and T have been estimated from count ratios between B1 and B3 using the Count Rate Prediction Program (Van Beek et al., 1981).

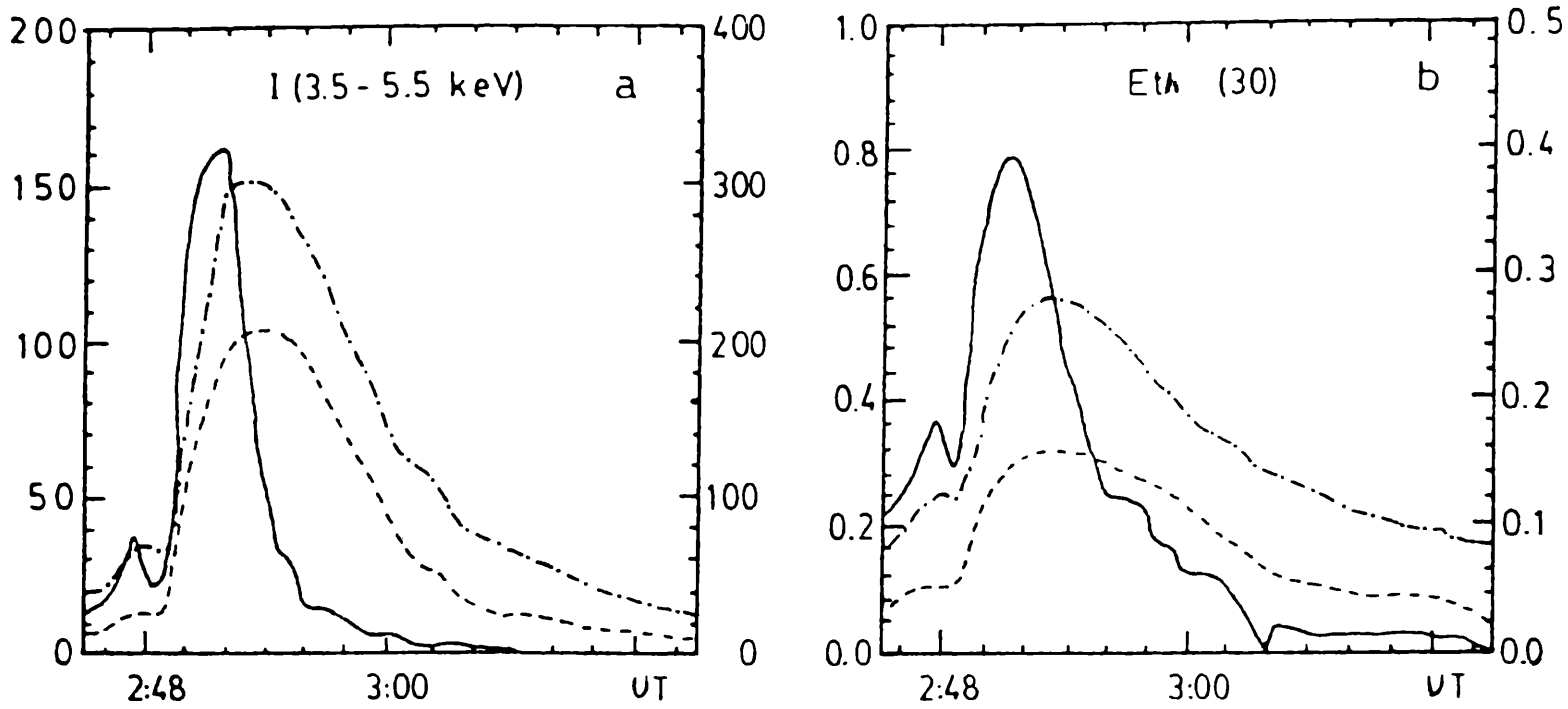

Fig. 10 Nov. 12, 02:42 UT flare. a) and b) idem Fig. 8 a) and b).

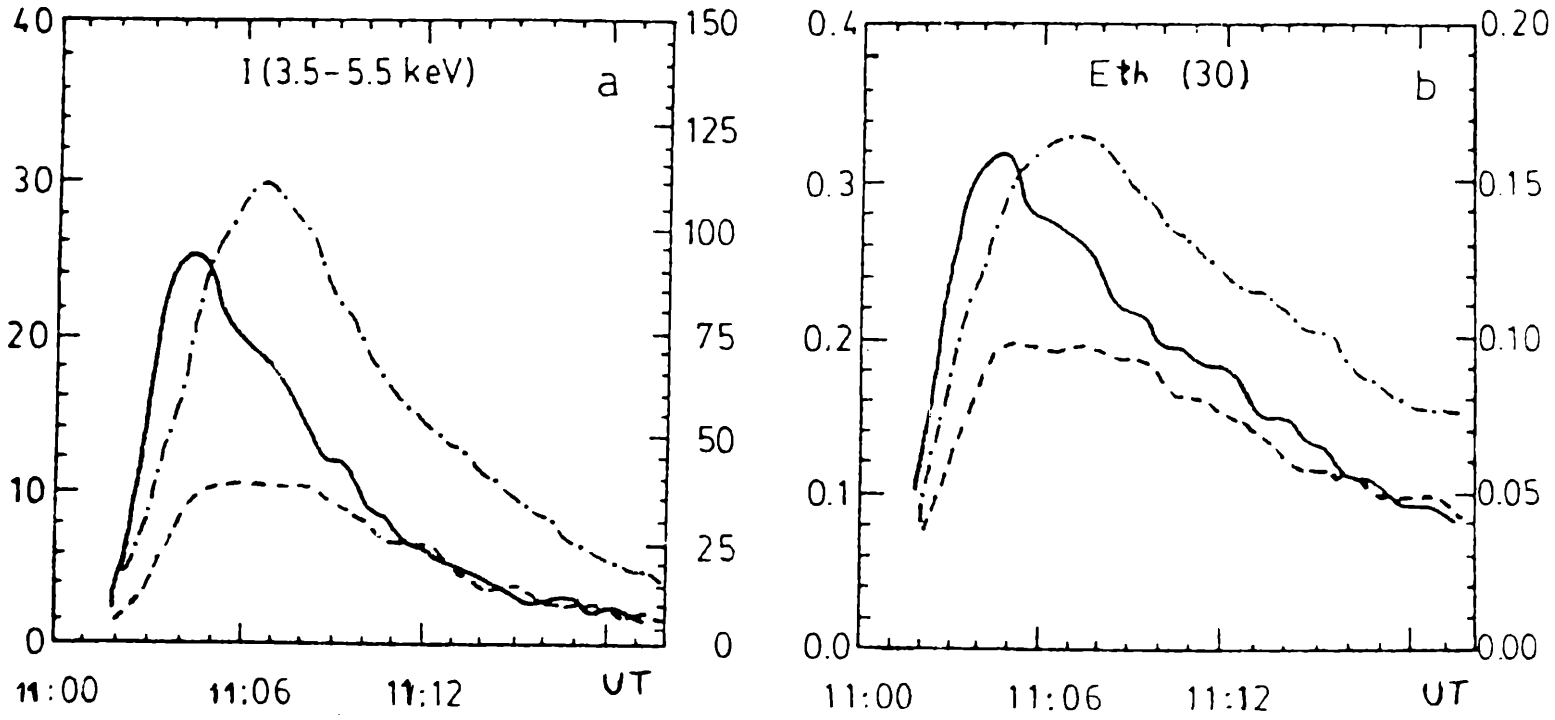

Fig. 11 Nov. 12, 11:00 UT flare. a) Idem Fig. 8 a), corresponding left vertical axis to F1 and right to F2 and F3. b) Idem Fig. 9 b).

Bearing in mind our working premise, the facts that: bipole F2 is the seat of the gradual phase of the hard X-ray burst, develops its Eth in agreement with this hard X-ray emission, is energetically predominant in the time integrated output and is located over a neutral line with observable magnetic shear

extending towards a strong field region, compel the conclusion that the bulk of the energy release in these flares took place within this structure. On the other hand, the instability that triggered the phenomenon seems to start either within F1 or at the interaction site between bipoles where the X-ray nucleus is observed during the onset phase. F1 is the seat of intense magnetic shear and its hard X-ray emission and Eth dominates during this period, suggesting that some energy release also occurs here in close association with the production of high energy particles.

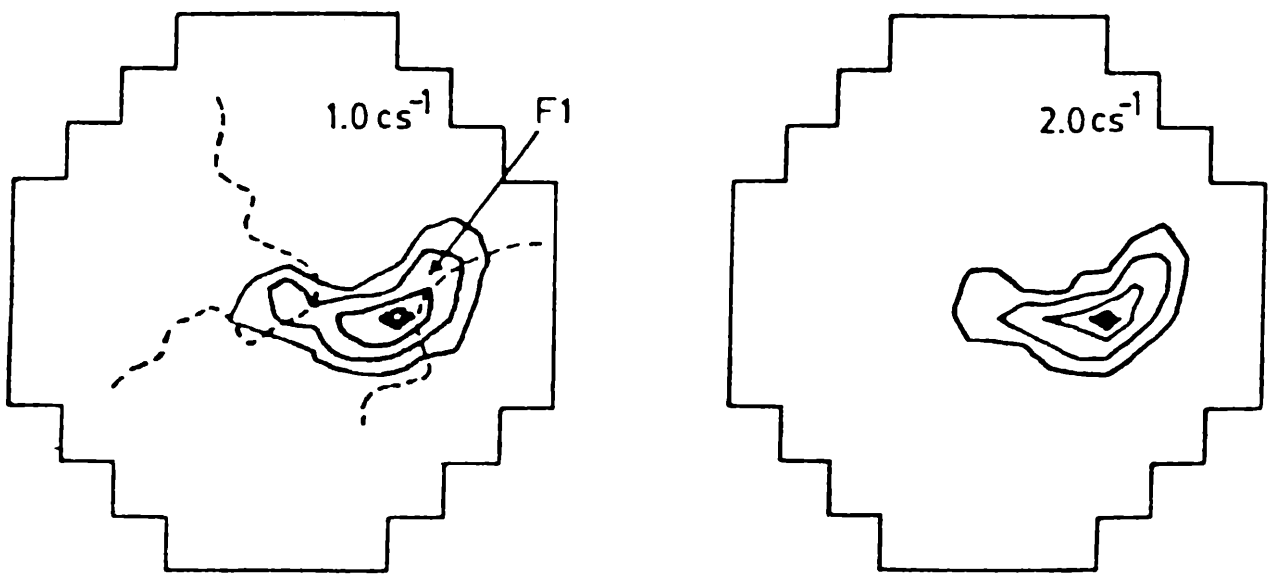

Fig. 12 16 - 30 keV images of HXIS FFOV for Nov. 11 flare. Contours are 90, 75, 50, 25 and 10% of maximum intensity.

While bipole F3, contrary to F1 and F2, has little shear and no appreciable hard X-ray emission indicating that this structure receives most of its energy from the others rather than from its own internal content. When internally stored energy is released within a bipole, we call it active and, in the opposite case, we call it passive. According to this, F1 and F2 are active structures and F3 is passive.

A series of flares that developed from April 7 to 10, 1980 in AR 2372 presented similar characteristics as those just described (Machado et al, 1983; Machado, 1985; Machado et al., 1988a). The magnetic configuration of AR 2372 was also composed of two main spots and a reversed polarity region in between; a sketch as the one in Figure 4c is also suitable for this region. In this particular case, the MSFC coverage during 4 days with little foreshortening allowed an accurate estimate of the evolution of the transverse field. It was observed that while the bipole over neutral line A was the site of persistent shear, neutral line regions B and C showed varying degrees of deformation from potential with time.

HXIS X-ray images show that during this period the energy release in AR 2372 flares began and spread among the different bipoles according to their relative shear, evolving as the relative magnetic stress did. In all cases the onset of the X-ray flare took place at the location of a small bipole; either over neutral line A from April 7 to 8 or a small loop across neutral line B on April 10, this was close to the larger loops over B (Machado et al., 1982; Machado and Moore, 1987). The impulsive phase was characterized by the expansion of the X-ray emission into bipoles over neutral lines B and C, being one of these the most important source during the gradual phase and changing predominance according to the magnetic evolution. During the impulsive phase chromospheric footpoints were observed in some of the

interacting bipoles, having this component the hardest spectrum; these facts indicate the presence of energetic electrons. In this case also Eth(t) for the three structures (see e.g. Fig. 5 for April 8, 02:57 UT event in Machado et al., 1988a) evolved in a similar way as in the November flares; being the small bipole predominant during the flare onset phase and dominating one of the other structures the thermal energy content of the whole flare, while the third behaved as a passive bipole.

A common characteristic, to both November and April flares, was the slow brightening of the global bipole of the active region (structure D in Fig. 4c). Figures 13 and 14 show the spatial evolution of a large scale structure in HXIS images after the November flares and the April 7, 05:27 UT event. In a magnetic configuration like the one of AR 2779 and AR 2372, the natural site for reconnection and particle injection into different structures is at the X-type neutral point depicted in Figure 4c (see theoretical work by Syrovatskii, 1969a,b, 1972, 1982).

Flare associated large scale (> 10^{10} cm) X-ray brightenings, the so-called "giant arches", were discovered in HXIS images hours after the onset of the ejective flare of May 21, 1980 (Svestka et al., 1982a). In this and following studies (Švestka et al., 1982b; Švestka, 1984; Hick and Švestka, 1985, 1987; Hick et al., 1987) it was shown that giant arches appeared after two-ribbon flares and it was inferred that both phenomena were due to a common underlying physical model. In a recent work (Mandrini and Machado, 1990) we have shown that large scale loop brightenings are observed in a large variety of situations, of which the events just described are an example, being not uniquely related to two-ribbon flares. Furthermore, our analysis shows that when large scale structures are observed in association with ejective events, they appear in a topologically distinct set of magnetic loops than those that give raise to the classical (post)flare loops. Our results suggest that this large brightenings, not only in

confined flares but also in ejective flares, are pre-existing coronal systems of loops energized by the underlying flare. The observation of similar phenomena in different classes of flares (confined and ejective) emphasize the global character of energy release in the magnetic structures of an active region.

We have been presenting up to now an scenario for flare occurrence in which impacted bipoles participate in the events, being the interaction closely associated with the impulsive energy release, but coming the bulk of the energy from the internal repository within these structures. Other interesting examples from the original list are the May 9, July 14 and May 21, 1980 flares. The first is a confined flare, the second one can be classified as a composite of confined and ejective and the third is a typical two-ribbon event.

May 9, 1980 flare from AR 2418 (Doscheck et al., 1981; Antonucci, 1982; Machado et al., 1988a,b) was composed of two interacting bipoles; one was observed as a compact and bright feature and the other as a large and dim structure. The smaller bipole was located over a neutral line showing intense shear, at both sides of which chromospheric footpoints appeared during the impulsive phase. This site was also characterized by a strong total vector field. The large X-ray structure was a system of loops (see Fig. 10 in Machado et al., 1988a) extending from one of the footpoints of the compact bipole into a region of weak field. Machado et al. (1988b) detected two X-ray fronts moving from the bright source along these loops; according to their estimates these fronts might have been originated during the strongest hard X-ray peak. Besides, the analysis of the thermal energy content of each bipole shows that most of the flare energy was released within the small region; while the large loops passively received energy injected from the X-ray kernel.

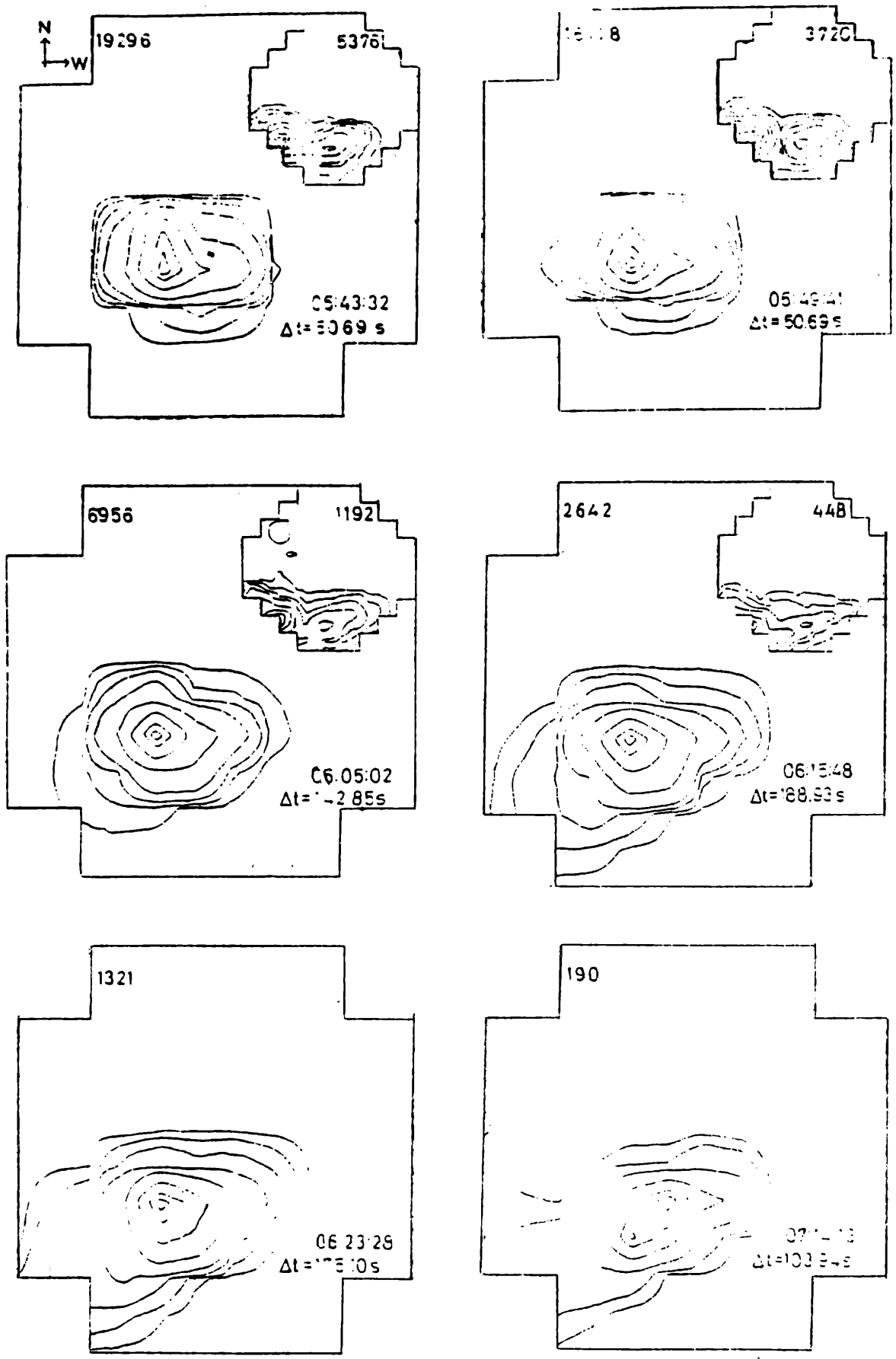

Fig. 13 Soft X-ray contours (3.5 - 8.0 keV) showing the development of a large scale structure in the HRIS fields of view after April 7, 05:27 UT flare. The FFOV has been superimposed on the upper right corner of the CFOV, in this last case every step is equal to 64' on the Sun. The contours correspond to: 90, 75, 50, 25, 10, 5, 2.5 and 1% of the maximum number of counts which is noted on the top of each field. The mean times (UT) and the integration intervals (t) are shown in the lower part of every image.

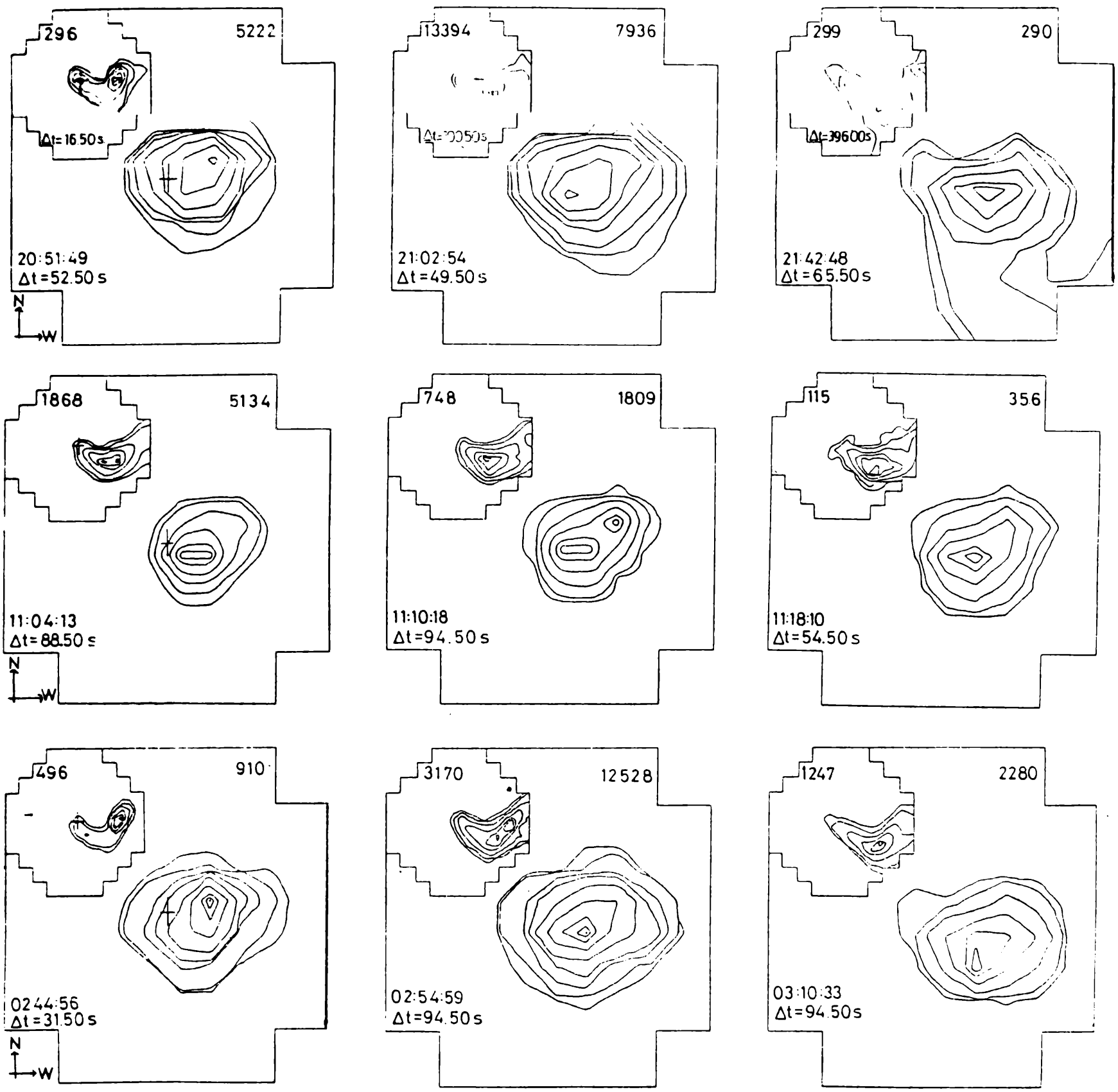

Fig. 14 Soft X-ray (3.5 - 8.0 keV) time evolution of a large scale feature after the three flares observed in AR 2779 on Nov. 11 (top) and Nov.12, 11:00 UT (center) and 02:42 UT (bottom). The contour levels are equal to those in Fig. 13 and the numbers within each field correspond to the same parameters; note that in the Nov. 11 event t is different for both fields of view.

July 14, 1980 flare in AR 2562 also comprised two interacting bipoles. The X-ray and Hα development of this flare (Fig. 12 in Machado et al., 1988a) shows a small nucleus and an extended configuration of two-ribbon type. The main difference between this event and the one mentioned before, is that both structures present an independent, but quantitatively comparable, thermal energy evolution. This, along with a filament eruption in the large system of loops, indicates that stored magnetic energy was released in this structure.

We refer now to the well-studied two-ribbon flare on May 21, 1980 in AR 2456 (see de Jager and Svestka, 1985 for a review) as another example of interaction between bipoles in a different type of event. Prior to the flare impulsive phase (35 m) new magnetic flux was observed in the longitudinal magnetograms obtained at the Kitt Peak National Observatory (Harvey, 1983). Hoyng et al. (1981) proposed that the emergence of this small bipole was the likely cause of the destabilization of the AR filament (see the emergence flux model, Heyvaerts et al., 1977). The X-ray emission from this region, which was the site of a hard X-ray footpoint at the time of the impulsive peaks (Duijveman et al., 1982), evolved in a different time scale than that of the large bipole above which the filament was located, showing its individual character. On the other hand, the gradual hard X-ray component was observed high in the corona at the top of the growing system of (post)flare loops; these dominated the thermal energy content of the flare (Duijveman, 1983).

The results just described confirm the picture presented in the case of more complex events. More examples and/or more details on the events in this Section can be found in Table I of Machado et al. (1988a) and references therein.

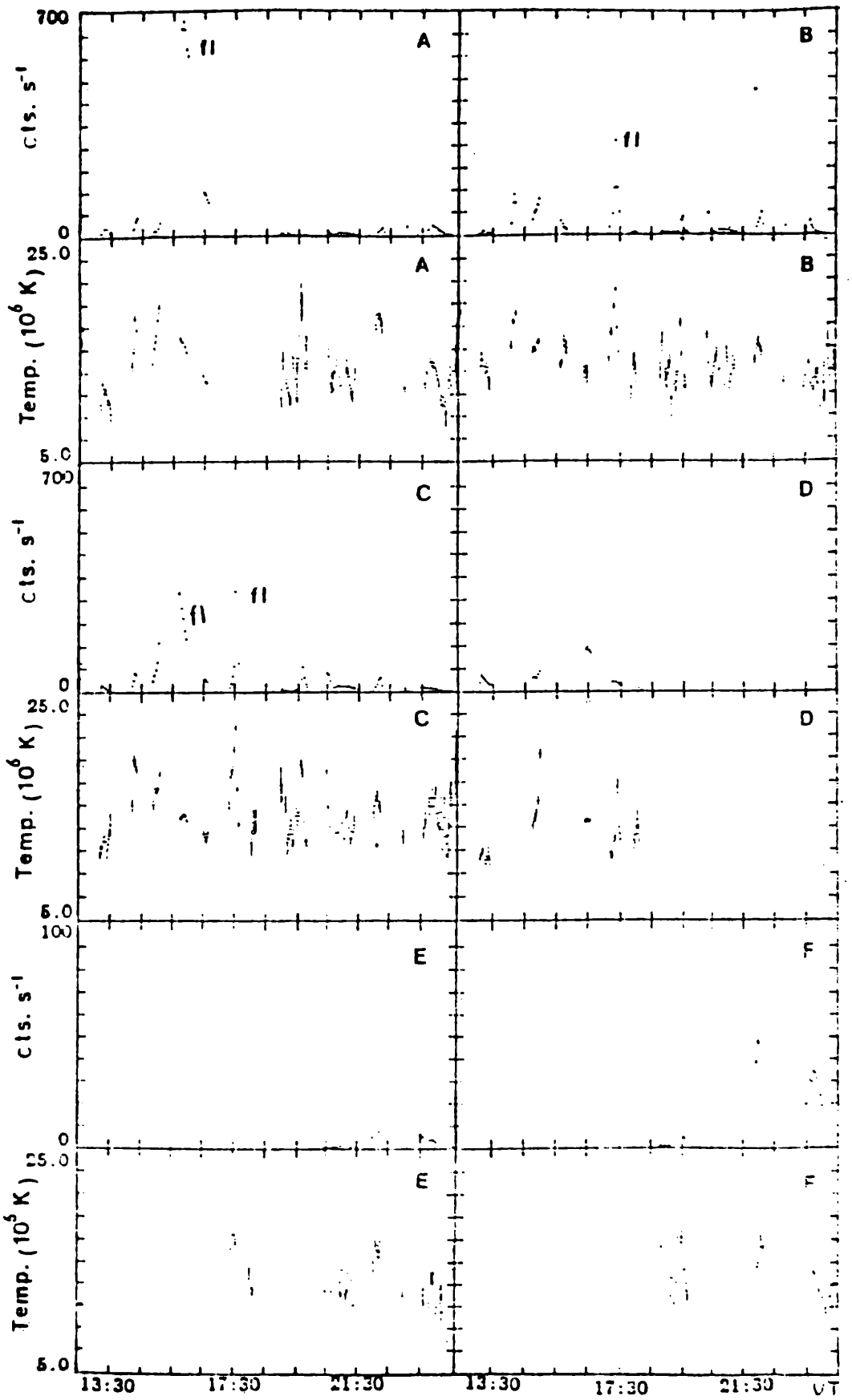

Fig. 15 3.5 - 5 keV intensity ant temperature as a function of time for the different brightenings observed in AR 2779 on Nov. 6 (see Fig. 16). Letters fl indicate the flares.

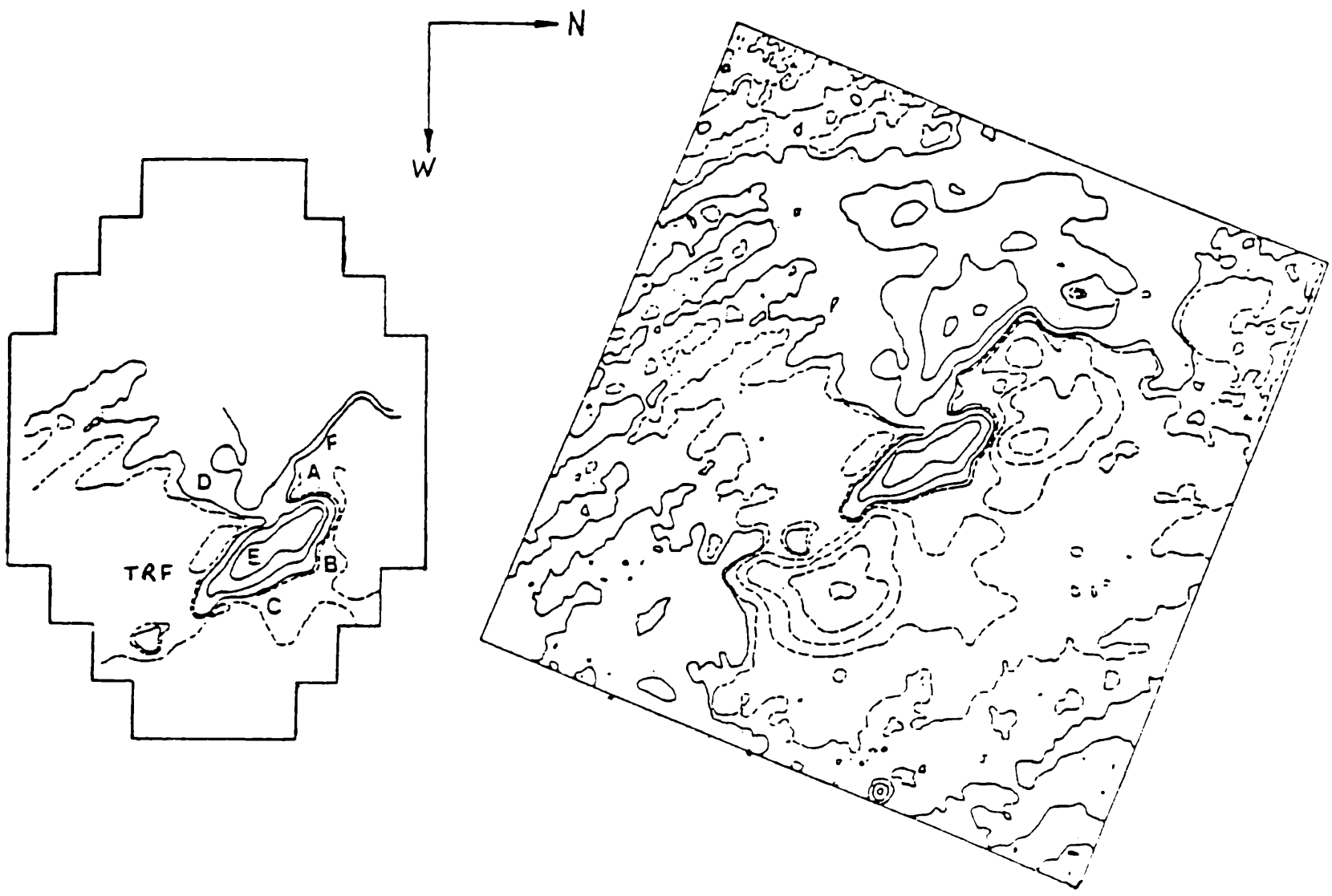

Fig. 16 Longitudinal magnetogram of AR 2779 (right). On the left we show within HXIS FFOV the position of: kernels A and B, the two-ribbon flare (TRF) and, approximately, that of the other brightenings.

2.2 Microflares

We turn now to the study of weak flare-like transient brightenings, often called "microflares", and then put this in perspective with the flares analyzed previously. These phenomena, detected for the first time in HXIS data by Schadee et al. (1983), are observed frequently and simultaneously in active regions. Here, we describe briefly HXIS observations of AR 2779 along 12 h on Nov. 6, 1980 (Mandrini et al., 1989).

Figure 12 (top) shows approximately the configuration in which the brightenings took place. This magnetogram was obtained on Nov. 7, 1980 when foreshortening effects did not render the magnetic observations unreliable. The soft X-ray intensity and the thermal evolution for the different events are depicted in Figure 15. The plots in this figure correspond to several zones in the AR, whose location has been indicated in Figure 16. Here we show HXIS FFOV stretched in the E - W direction to compensate foreshortening differences between Nov. 6 (X-ray observations) and 7 (magnetic data). In Figure 15 we have omitted the contribution of an ejective event that developed towards the SE and whose position is shown as TRF in Figure 16. The numerous weak brightenings that occurred during this day had peak intensities of several tenths in HXIS observations (Fig. 15). In the HXIS count rate scale a small to medium size flare (type B or C in the X-ray classification, see e.g. Švestka, 1976) reaches a maximum of several hundreths to 1000 c s , while larger events (type M or X) show peak intensities above the last value. It can be seen that, in spite of their weakness, T in these zones during microflares are between 10 K and 2 10 K which are typical of more important flares.

In Figure 17 we present a set of soft X-ray images in which the morphology of flares and microflares can be appreciated. The three contours in the second row show flares in progress. The first

two correspond to the evolution of the growing system of (post)flare loops after Nov. 6, 14:44 UT two-ribbon flare; notice the soft X-ray kernel in A simultaneously. Figure 17f, on the other hand, is an image of a confined flare that started at 17:25 UT and which comprises two magnetic structures (Mandrini, 1989): a compact bipole B and a large bipole C, in agreement with the general picture of multiple loop flare topologies as discussed before.

The recurrent pattern of activity observed in the images is particularly remarkable. Regions A and B, along a neutral line with intense magnetic shear (see Fig. 3), are the sites of repeated X-ray emission of varied intensity. The fact we want to emphasize is that the shape of the emitting regions is preserved notwithstanding differences in intensity among events, compare contours in Figure 17f for the flare with weak brightenings in 17c, h and i. That is to say, the global morphology of two bipoles does not change no matter the brightness ratio between flares and microflares.

We have also found that averaging over the period of our observations, the brightenings imply a mean energy input rate of $\simeq 10^{26}$ erg s^{-1} which is enough to heat the active region corona (see also Lin et al., 1984).

The similitude in the X-ray emission observed during flares and microflares suggests very strongly that both phenomena are driven by the same basic physical process. That is to say, interaction between impacted bipoles triggers the event and induces the release of stored energy. The possibility of a common phenomenology between flares and microflares was discussed by Lin et al. (1984) and Athay (1984). We have found similar results for weak brightenings in AR 2372 (Hernandez et al., 1990).

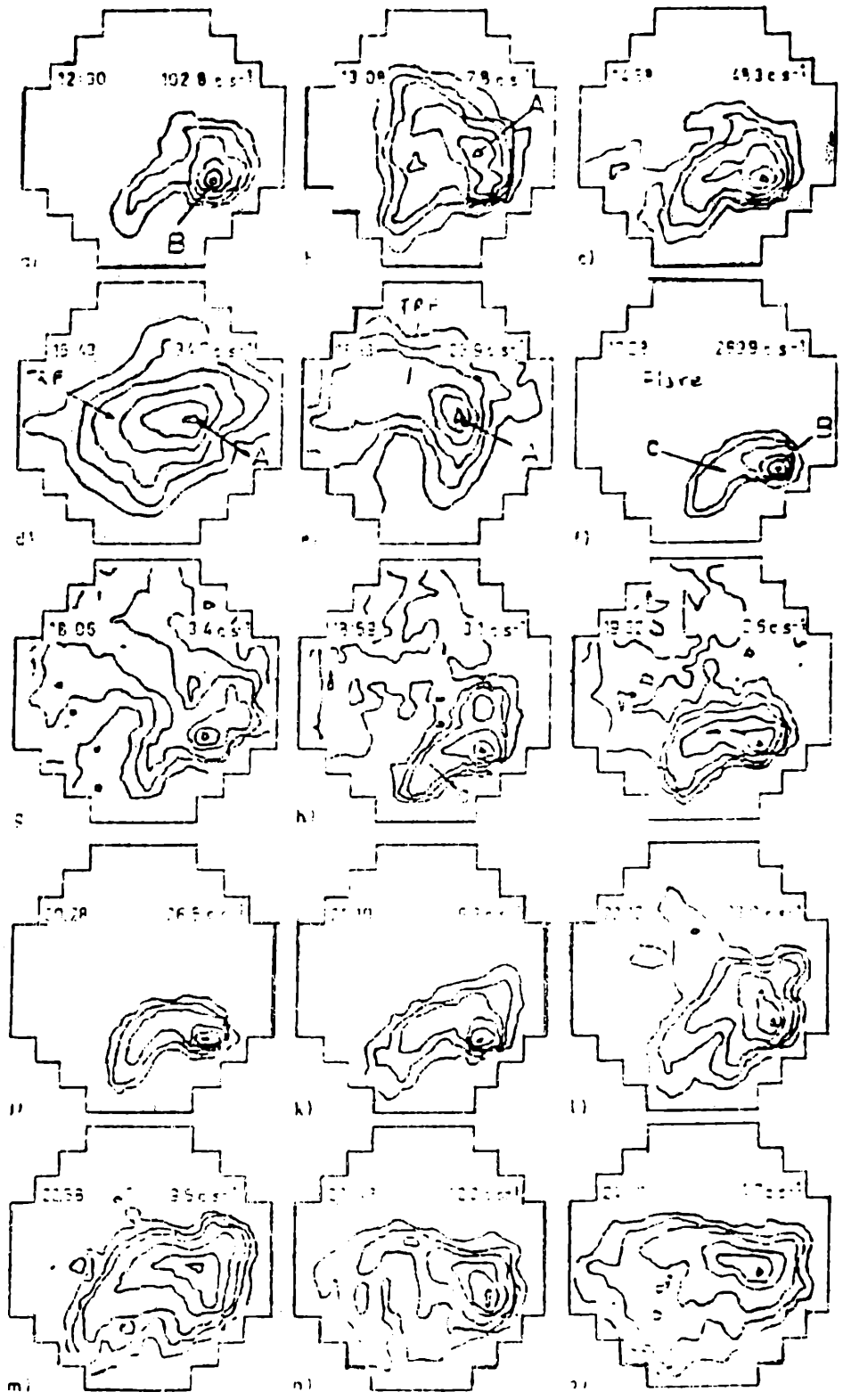

Fig. 17 Soft X-ray images (3.5 - 5 keV) at different times along the 12 hours of observation. The lowest intensity is equal to twice the instrumental background. We indicate the UT for every image (upper left corner) and the maximum number of c s-1 (upper right corner).

3. DISCUSSION

The observational properties presented in the previous Section lead us to the following picture. The basic structure of a flare consists of an initiating closed bipole plus one or more adjacent bipoles impacted against it. As far as our observations can tell, the energy release can begin either within the initiating magnetic structure or at the interaction site between them. There is ample evidence showing that the bipoles interact strongly in the impulsive phase, during which most of the energy is released inside one or more structures rather than at the interaction site. Besides, the strongest and most impulsive particle accceleration is closely associated with the loop system showing the greatest magnetic stress. If an adjacent bipole has stored energy (indicated by the product of the spatial extent, strength and degree of deformation from potential of its magnetic field) and is sufficiently unstable, the interaction can trigger energy release within it; on the other hand, if this does not happen or the structure is sufficiently stable, no energy is released within it but particles and/or heat can be injected from the interaction site.

The interaction between bipoles suggests the formation of an external current sheet and reconnection at the interface, triggering the impulsive production of energetic particles. Afterwards, our results indicate that the way in which a flare would evolve is characterized by the internal energy available in every bipolar region (see Fig. 14 in Machado et al., 1988a). That is to say, the responsability of releasing the flare energy does not rest on the external current sheet as in many flare models but on the loops themselves (see reviews on flare models mentioned before). The results derived from the analysis of microflares shows that this same scenario expands over a vast range of energies.

Our data are, on the other hand, compatible with previous well-established observational flare characteristics (see Section 1.1); mainly those concerning the association of flare activity with regions of high field gradient, as well as strong shear. They are also consistent with Skylab picture of coronal loops as the basic structure of flares, being in this case the main new findings: the importance of bipole interactions as the trigger mechanism for flares and other weak events and the lack of a clear physical distinction between confined and ejective events. In this last case we refer not only to common characteristics of energy release and triggering, but also to the possibility that both classes of events may encompass global magnetic structures in the active region. Our observations of large scale brightenings, associated to both types of flares, also show the importance of field connections as the building blocks of the energy release process.

Finally, we want to call the attention to the fact that all the examples from the original list in Machado et al. (1988a), to which we can add up microflares in AR 2779 (Mandrini et al., 1989) and in AR 2372 (Hernandez et al., 1990) and also giant arches in two-ribbon flares (see e.g. Nov. 6, 1980 event in Mandrini and Machado, 1990), encompassed more than one system of loops; meaning this that the picture of interacting bipoles seems to be a common scenario for these phenomena.

In fact, all these new results show that flares are not isolated self-contained phenomena in active regions. Their overall properties span several decades in all basic characteristics like: total energy output, power, brightness and temporal and length scale. The flare phenomenon is, thus, much more associated with the global properties of an active region than what previous results led us to believe.

ACKNOWLEDGEMENTS

We acknowledge M. Rovira for a thorough reading of the manuscript.

References

Antiochos, S.K.: 1987, Astrophys. J. **312**, 886.
Antonucci, E.: 1982, Mem. Soc. Astr. Italiana **53**, 495.
Athay, R.G.: 1984, Solar Phys. **93**, 123.
Athay, R.G. and Moreton, G.E.: 1961, Astrophys. J. **133**, 935.
Bell, B. and Glazer, H.: 1959, Smithson. Contrib. Astrophys. **3**, 4.
Birn, J. and Schindler, K.: 1981, in E.R. Priest (ed.), Solar Flares Magnetohydrodynamics, Gordon and Breach, N. Y., p. 337.
Brown, J.C., Melrose, D.B. and Spicer, D.S.: 1979, Astrophys. J. **228**, 592.
Carrington, R.C.: 1860, Month. Not. Roy. Astron. Soc. **20**, 13.
Cheng, C.-C., Pallavicini, R., Acton, L.W. and Tandberg-Hansen, E.: 1985, Astrophys. J. **298**, 887.
Chupp, E.L., Forrest, D.J., Highie, P.R., Suri, A.N., Tsai, C. and Dunphy, P.P.: 1973, Nature **241**, 5388.
Datlowe, D.W., Elcan, M.J. and Hudson, H.S.: 1974a, Solar Phys. **39**, 155.
Datlowe, D.W., Hudson, H.S. and Peterson, L.E.: 1974b , Solar Phys. **35**, 193.
De Jager, C. and Boelee, A.: 1984, Solar Phys. **92**, 227.
De Jager, C. and Svestka, Z.: 1985, Solar Phys. **100**, 435.
Dennis, B.R.: 1987, private communication.
Dodson, H.W. and Hedeman, E.R.: 1960, Astron. J. **65**, 51.
Dodson, H.W. and Hedeman, E.R.: 1970, Solar Phys. **9**, 278.
Doschek, G.A.: 1983a, Solar Phys. **86**, 9.
Doschek, G.A.: 1983b, Solar Phys. **86**, 48.

Doschek, G.A., Feldman, U., Landecker, P.B. and McKenzie, D.L.: 1981, Astrophys. J. **249**, 372.
Duijveman, A.: 1983, Solar Phys. **84**, 189.
Duijveman, A., Hoyng, P. and Machado, M.E.: 1982, Solar Phys. **81**, 137.
Dwivedi, B.N., Hudson, H.S., Kane, S.R. and Svestka, Z.: 1984, Solar Phys. **90**, 331.
Ellison, M.A., McKenna, S.M.P. and Reid, J.H.: 1961, Dunsink Obs. Publ. **1**, 53.
Emslie, A.G. and Machado, M.E.: 1987, Solar Phys. **107**, 263.
Gomez, D.O. and Ferro Fontan C.: 1988, Solar Phys. **116**, 33.
Hagyard, M.J.: 1988, Solar Phys. **115**, 107.
Hagyard, M.J., Smith, J.B.Jr., Teuber, D. and West, E.A.: 1984, Solar Phys. **91**, 115.
Harvey, J.W.: 1983, Adv. Space Res. **2** No. 11, 31.
Henoux, J.C. and Somov, B.V.: 1987, Astron. Astrophys. **185**, 306.
Hernandez, A.M., Rovira, M.G., Mandrini, C.H. and Machado, M.E.: 1990, Rev. Mex. Astron. Astrof., in press (abstract).
Heyvaerts, J., Priest, E.R. and Rust, D.M.: 1977, Astrophys. J. **216**, 123.
Hick, P. and Svestka, Z.: 1985, Solar Phys. **102**, 147.
Hick, P. and Svestka, Z.: 1987, Solar Phys. **108**, 315.
Hick, P., Svestka, Z., Smith, K.L. and Strong, K.: 1988, Solar Phys. **114**, 329.
Hodgson, R.: 1860, Month. Not. Roy. Astron. Soc. **20**, 15.
Hoyng, P., Brown, J.C. and Van Beek, H.F.: 1976, Solar Phys. **48**, 197.
Hoyng, P., Duijveman, H., Machado, M.E., Rust, D.M., Svestka, Z., Boelee, A. and 6 co-authors 1981, Astrophys. J. Let. **246**, L155.
Hudson, H.S., Peterson, L.E. and Schwartz, D.A.: 1969, Astrophys. J. **157**, 398. Kane, S.R.: 1983, Solar Phys. **86**, 355.
Kane, S.R. and Anderson, K.A.: 1970, Astrophys. J. **162**, 1003.

Kane, S.R., Anderson, K.A., Evans, W.D., Klebesadel, R.W. and Laros, J.: 1979, Astrophys. J. Let. **233**, L151.

Kondo, I.: 1983, in Proc. of Hinotori Symp. on Solar Flares, p. 3.

Krall, K.R., Smith, J.B.Jr., Hagyard, M.J., West, E.A., and Cummings, N.P.: 1982, Solar Phys. **79**, 59.

Kundu, M.R. and Woodgate, B. (eds.): 1986, Energetic Phenomena on the Sun, NASA CP 2439.

Kuperus, M., Ionson, J.A. and Spicer, D.A.: 1981, Ann. Rev. Astron. Astrophys. **19**, 7.

Lin, R.P., Schwartz, R.A., Kane, S.R., Pelling, R.M. and Hurley, K.C. 1984, Astrophys. J. **283**, 421.

Low, B.C.: 1982, Rev. of Geophys. and Spac. Phys. **20**, 145.

Machado, M.E.: 1982, Adv. Space Res. **2**, No 11, p. 115.

Machado, M.E.: 1985, Solar Phys. **99**, 159.

Machado, M.E., Duijveman, A. and Dennis, B.R.: 1982, Solar Phys. **79**, 85.

Machado, M.E. and Moore, R.L.: 1987, Adv. Space Res. **6**, p. 217

Machado, M.E., Moore, R.L., Hernandez, A.M., Rovira, M.G., Hagyard, M.J. and Smith, J.B.Jr.: 1987, Astrophys. J. **326**, 425

Machado, M.E., Somov, B.V., Rovira, M.G. and de Jager, C.: 1983, Solar Phys. **85**, 157.

Machado, M.E., Xiao, Y.C., Wu, S.T. Prokakis, Th. and Dialetis, D.: 1988b, Astrophys. J. **326**, 451.

Mandrini, C.H.: 1989, Thesis, University of Buenos Aires.

Mandrini, C.H., Machado, M.E., Hernandez, A.M. and Rovira, M.G.: 1989, Adv. Sp. Res. **10**, No 9, 115.

Mandrini, C.H. and Machado, M.E.: 1990, Solar Phys., submitted.

Martres, M.J. and Pick, M.: 1962, Ann. Astrophys. **25**, 4.

Martres, M.J., Michard, R. and Soru-Iscovici, I: 1966, Ann. Astrophys. **29**, 249.

McClymont, A.N. y Fisher, G.H.: 1989, Amer. Geophys. Union Mon.

Moore, R.L., McKenzie, D.L., Svestka, Z., Widing, K.G., Antiochos, S.K., Dere, K.P. and 10 co authors: 1980, in P.A. Sturrock (ed.), Solar Flares - A Monograph from Skylab Workshop II, Colorado Associated University Press, Chap. 7.

Moreton, G.E. and Ramsey, H.E.: 1960, Publ. Astron. Soc. Pacific **72**, 357.

Moreton, G.E. and Severny, A.B.: 1968, Solar Phys. **3**, 282.

Neidig, D.F. 1977, Solar Phys. **54**, 165. Orrall, F.Q. (ed.): 1981, Solar Active Regions, Colorado Associated University Press.

Orwig, L.E., Frost, K.J. and Dennis, B.R.: 1980, Solar Phys. **65**, 25.

Pallavicini, R., Serio, S. and Vaiana, G.S.: 1977, Astrophys. J. **216**, 108.

Parker, E. N.: 1981 a, Astrophys. J. **244**, 631.

Parker, E. N.: 1981 b, Astrophys. J. **244**, 644.

Parker, E. N.: 1983 a, Astrophys. J. **264**, 635.

Parker, E. N.: 1983 b, Astrophys. J. **264**, 642.

Priest, E.R.: 1982, in E.R. Priest (ed.), Solar Magnetohydrodynamics, D. Reidel Pub. Co., Dordrecht, p. 1.

Ramaty, R., Kozlovsky, B. and Lingenfelter, R.E.: 1975, Space Scie. Rev. **18**, 341.

Richardson, R.S.: 1951, Astrophys. J. **114**, 356.

Richardson, R.S.: 1936, Annual Rep. Director Mt. Wilson Obs. **35**, 871.

Rovira, M.G.: 1990, Rev. Mex. Astron. Astrof., in press.

Schadee, A., de Jager, C. and Sveetka, Z.: 1973, Solar Phys. **89**, 287.

Smith, D.F. and Lilliequist, C.G.: 1979, Astrophys. J. **232**, 582.

Spicer, D.S.: 1977, Solar Phys. **53**, 305.

Spicer, D.S. and Brown, J.C.: 1981, in S. Jordan (ed.), The Sun as a Star, NASA SP-450, p. 413.

Sturrock, P.A. (ed.): 1980a, Solar Flares - A Monograph from Skylab Workshop II, Colorado Associated University Press.

Sturrock, P.A.: 1980b, in P.A. Sturrock (ed.), Solar Flares - A Monograph from Skylab Workshop II, Colorado Associated University Press, p. 411.

Švestka, Z.: 1968, in K.O. Kiepenheuer (ed.), Structure and Development of Solar Active Regions, D. Reidel Pub. Co., Dordrecht, p. 513.

Švestka, Z.: 1976, Solar Flares, D. Reidel Pub. Co., Dordrecht.

Švestka, Z.: 1981, in E.R. Priest (ed.), Solar Flare Magnetohydrodynamics, Gordon and Breach Scie. Pub., London, p. 47.

Švestka, Z.: 1984, Solar Phys. **94**, 171.

Švestka, Z.: 1984b, Adv. Sp. Res. **4** No. 7, 179. Svestka, Z.: 1986, in D.F. Neidig (ed.), The Lower Atmosphere of Solar Flares, Sunspot, N.M., National Solar Observatory, p. 332.

Švestka, Z., Dennis, B.R., Pick, M. Raoult, A. Rapley, C.G., Stewart, R.T. and Woodgate, B.E.: 1982b, Solar Phys. **80**, 143.

Švestka, Z., Kopecky, M. and Blaha, M.: 1961, Bull. Astron. Inst. Czech. **12**, 229. Svestka, Z., Stewart, R.T., Hoyng, P., Van Tend, W., Acton, L.W., Gabriel, A.H. and 10 co-authors: 1982a, Solar Phys. **75**, 305.

Syrovatskii, S.I.: 1969a, in C. de Jager and Z. Svestka (eds.), Solar Flares and Space Research, North-Holland, Amsterdam, p. 346.

Syrovatskii, S.I.: 1969b, Trudy Mezhdunar Seminara, Leningrad p. 7.

Syrovatskii, S.I.: 1972, in C. de Jager (ed.), Solar - Terrestrial Physics, **Part I**, p. 119.

Syrovatskii, S.I.: 1982, Solar Phys. 76, 3.

Tanaka, K. and Nakagawa, Y.: 1973, Solar Phys. **33**, 187.

Tanaka, K.: 1983, Solar Phys. **86**, 3.

Tanaka, K.: 1987, Publ. Astron. Soc. Japan **39**, 1.

Valnicek, B.: 1961, Bull. Astron. Inst. Czech. **12**, 237.

Van Ballegooijen, A. A.: 1986, Astrophys. J. **311**, 1001.

Van Beek, H. F.: 1973, Thesis, University of Utrecht.

Van Beek, H. F., de Jager, C., Fryer, R., Schadee, A., Svestka, Z., Boelee, A. and 18 co-authors: 1981, Astrophys. J. Let. **244**, L157.

Van Beek, H.F., Hoyng, P., Lafleur, B. and Simnett, G.M.: 1980, Solar Phys. **65**, 39.

Van Hoven, G.: 1976, Solar Phys. **49**, 95.

Van Hoven, G.: 1981, in E.R. Priest (ed.), Solar Flare Magnetohydrodynamics, Gordon and Breach, New York, p. 217.

Vlahos, L., Machado, M.E., Ramaty, R., Murphy, R.J., Alissandrakis, C., Bai, T. and 21 co-authors: 1986, in Kundu M. y Woodgate B. (eds.), Energetic Phenomena on the Sun, NASA CP-2439, Chap. 2.

Waldmeier, M.: 1938, Z. Astrophys. **15**, 299.

Wang, H.T. and Ramaty, R.: 1974, Astrophys. J **202**, 532.

White, W.A.: 1964, in AAS-NASA Symp. on the Physics of Solar Flares, NASA Scient. and Tech. Inf. Div., p. 131.

Wood, A.T. Jr., Noyes, R.W., Dupree, A.K., Huber, M.C.E., Parkinson, W.H., Reeves, E.M. and Withbroe, G.L.: 1972, Solar Phys. **24**, 169.

Wood, A.T. Jr. and Noyes, R.W.: 1972, Solar Phys. **24**, 180.

Zvereva, A.M. and Severny, A.B.: 1970, Izv. Krymsk. Astrofiz. Obs. **41**, 97.

Zirin, H. and Tanaka, K.: 1973, Solar Phys. **32**, 173.

Zirker, J. (ed.): 1977, Coronal Holes and High Speed Solar Wind Streams, Colorado Associated University Press.